Vehicle following control for cornering maneuvers with vehicle platoons

Schoenmakers, R.M.

Award date:
2022

EINDHOVEN UNIVERSITY OF TECHNOLOGY

Department of Mechanical Engineering
Dynamics and Control Research Group
Master Automotive Technology

Vehicle following control for cornering maneuvers with vehicle platoons

Master Thesis Report

DC 2022.007

R.M. Schoenmakers
0911399

Supervisors:
Prof. Dr. H. Nijmeijer
Dr. Ir. T. van der Sande
Ir. W. Schinkel

Eindhoven, March 2022

Declaration concerning the TU/e Code of Scientific Conduct for the Master's thesis

I have read the TU/e Code of Scientific Conduct[i].

I hereby declare that my Master's thesis has been carried out in accordance with the rules of the TU/e Code of Scientific Conduct

Date

07-03-2022

Name

R.M. Schoenmakers

ID-number

0911399

Signature

R. Schoenmakers

Submit the signed declaration to the student administration of your department.

[i] See: https://www.tue.nl/en/our-university/about-the-university/organization/integrity/scientific-integrity/
The Netherlands Code of Conduct for Scientific Integrity, endorsed by 6 umbrella organizations, including the VSNU, can be found here also. More information about scientific integrity is published on the websites of TU/e and VSNU

Summary

The goal of this project is to develop an extended look-ahead controller for longitudinal and lateral vehicle tracking, which improves tracking performance during cornering maneuvers. This controller should maintain the path length between the vehicles independent of whether the platoon is driving straight or cornering. With the developed controller the length of the path between the vehicles equals the inter-vehicle distance as prescribed by the constant time-gap spacing policy for both driving straight and cornering.

The effectiveness of the developed controller is demonstrated by both simulations and experiments with the Renault Twizy. Simulations show that the developed controller successfully compensates for corner-cutting behaviour, while it maintains the length of the path between the vehicles during cornering. Experiments with two modified Renault Twizys are performed for the already existing extended look-ahead controller and the developed controller. Both controllers are implemented on the Renault Twizys and experimental results show that both controllers perform equally well on these vehicles. However, the simulation results prove that the developed extended look-ahead controller improves tracking performance during cornering maneuvers, since corner-cutting behaviour is compensated and the length of the path between the vehicles is maintained.

Preface

First of all, I would like to thank my supervisor Prof. Dr. Henk Nijmeijer. Thanks for your constant guidance throughout this graduation project. During our meetings you helped me improving my work by pointing out the weak points of my project. Your insights were crucial and really helped me making progress and pushed my project to a higher level.

I would also like to thank my supervisors Dr. Ir. Tom van der Sande and Ir. Wouter Schinkel. You gave me valuable feedback throughout this graduation project and this really improved the quality of my work. Thanks for the constant guidance and being patient with me at every step. Your support means a lot to me. Although most of our meeting were Teams meetings due to the COVID-19 pandemic, I really enjoyed those meetings nonetheless. I really enjoyed working in the AES lab on the Renault Twizys together. This gave me the opportunity to work on the campus during the pandemic and this really renewed my motivation.

I would also like to thank Dr. Ir. Erjen lefeber and Dr. Ir. Anggera Bayuwindra for providing me additional support during my graduation project. I have benefited greatly from your mathematical knowledge and thank you for taking the time for our meetings.

Thanks to all my friends for always being a source of companionship and support, especially during the pandemic.

Finally, I would like to thank my parents, Ton and Nicolle Schoenmakers, and my girlfriend, Maartje Rops, for always supporting me. Your support helped me to fully focus on my studies, but more importantly you provided me happy distractions outside my research.

Roy Schoenmakers

Contents

List of Symbols

Symbol	Description	Unit
α_i	Angle of arc	Rad
θ	Heading angle of the vehicle	Rad
θ_i	Heading angle of vehicle i	Rad
κ_{i-1}	Path curvature of vehicle $i-1$	1/m
ω_i	Angular velocity of vehicle i	Rad/s
ω_z	Angular velocity of the vehicle	Rad/s
a	Distance from the center of gravity to the front wheel	m
a_i	Longitudinal acceleration of vehicle i	m/s^2
b	Distance from the center of gravity to the rear wheel	m
C_1	Cornering stiffness of the front wheel	N/rad
C_2	Cornering stiffness of the rear wheel	N/rad
c_i	Varying time-gap constant	-
d_i	Inter-vehicle distance	m
$d_{r,i}$	Desired inter-vehicle distance	m
$d_{rx,i}$	x-component of the desired inter-vehicle distance	m
$d_{ry,i}$	y-component of the desired inter-vehicle distance	m
e_θ	Heading angle error	Rad
e_i	Spacing error	m
$e_{x,i}$	x-component tracking error	m
$e_{y,i}$	x-component tracking error	m
$h_{0,i}$	Varying time-gap constant	-
h_i	Time-gap	s
i	Index number	-
K	Number of samples	-
k_1	Controller gain	-
k_2	Controller gain	-
L	Look-ahead distance	m
L_i	Length of vehicle i	m
l	Wheelbase of the vehicle	m
l_a	Look-ahead distance	m
m	Mass of the vehicle	kg
p_i	Position of vehicle i	(m,m)
q	Distance between the linear approximation of the center-line of the lane and the center of gravity of the vehicle	m
R	Turning radius of the vehicle	m
R_{1r}	Virtual reference point lead vehicle	(m,m)
R_{2f}	Virtual reference point following vehicle	(m,m)
R_{i-1}	Turning radius of vehicle $i-1$	m
r_i	Standstill distance	m
S	Extended look-ahead point	(m,m)
s_{i-1}	Extended look-ahead point of vehicle $i-1$	(m,m)

$\bar{s}_{i-1}$	Magnitude of extended look-ahead point of vehicle $i-1$	m
$s_{x,i-1}$	x-component extended look-ahead point of vehicle $i-1$	m
$s_{y,i-1}$	y-component extended look-ahead point of vehicle $i-1$	m
t	Time	s
V	Longitudinal velocity of the vehicle	m/s
v_i	Longitudinal velocity of vehicle i	m/s
$v_{r,i}$	Relative velocity of vehicle i	m/s
v_x	Longitudinal velocity of the vehicle	m/s
x	x-position of the vehicle	m
x_i	x-position of vehicle i	m
y	y-position of the vehicle	m
y_i	y-position of vehicle i	m
y_{fb}	Feedback output approximation	m

Chapter 1

Introduction

1.1 Background

Vehicle platooning is a technique that is developed to improve traffic safety and highway capacity [1]. This is a term for cooperating vehicles driving in the form of a string, which are following each other at a short distance. In 88% of the traffic accidents with casualties the human driver caused the accident [2]. Traffic accidents caused by human errors, which include fatigue, tailgating and reaction time could be reduced by using vehicle automation [3]. Besides the safety aspect of driving the fuel efficiency is an important aspect where improvements are possible. In [4] it is shown that for trucks driving at a distance of 3 meters, the fuel consumption is reduced with 5% for the leading truck and that a reduction up to 15% is possible for the follower truck.

A solution for these problems is vehicle platooning. In vehicle platooning the longitudinal motion and optionally the lateral motion of a vehicle are automated. A vehicle platoon is able to increase the road capacity, since the vehicles are following each other at a short distance. A vehicle platoon consists of a lead vehicle, which is typically human driven, and automated follower vehicles [1]. For the automation of the longitudinal motion of the vehicle the techniques used in Adaptive Cruise Control (ACC) could be utilized. Here a radar, camera or lidar is used to determine the distance to the preceding vehicle and automatically accelerate or brake the vehicle to keep the prescribed distance. An enhanced version of ACC is Cooperative Adaptive Cruise Control (CACC), where vehicle-to-vehicle communication is used to obtain information such as speed and acceleration of the preceding vehicle. For the automation in the longitudinal direction of the vehicle different inter-vehicle distances could be used, here the reference is obtained from spacing policies.

For the automation of the lateral motion of the vehicle various strategies are described in literature. In this report two different approaches are considered, which are path following and direct vehicle following. With the path following method the vehicle follows a predefined path, while the direct vehicle method tracks and follows a preceding vehicle as can be seen in Figure 1.1. The path following method is implemented in [5], [6] and [7] and the vehicles successfully follow the predefined paths by using magnetic markers in the lanes of the roads, an RTK-GPS (Real Time Kinematic Global Positioning System) or a camera based vision system.

Another possibility is to follow a vehicle directly instead of following a predefined path. With this approach path information is not needed, but the drawback of this approach is that the vehicles in the platoon may cut corners [1]. To compensate for this corner cutting behaviour several strategies are developed which use a virtual tracking objective linked with the rear of the preceding vehicle, this point is the reference for the follower vehicle. When the follower vehicle follows this reference point, the corner cutting behaviour is compensated [1], [8]. In [1] an extended look-ahead controller is designed to compensate for the corner-cutting behaviour.

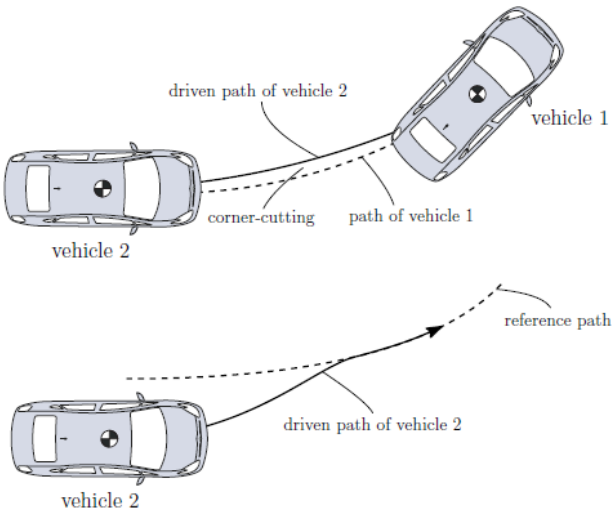

Figure 1.1: The vehicle following approach (top) and the path following approach (bottom) [1].

1.2 Problem statement and research objectives

In [5], [6] and [7] it is shown that the path following approach for longitudinal and lateral control of a vehicle platoon can be successfully implemented. The drawback of this technique is that it does not work when road markings are not visible for the camera vision system or information about the path is not available. Therefore, the direct vehicle method can be used for longitudinal and lateral control of the vehicle platoon, but this method has some drawbacks during cornering maneuvers, which includes the corner-cutting behaviour [1]. To prevent corner-cutting an extended-look ahead controller can be used, but with this controller the length of the path between the vehicles in the platoon decreases during cornering maneuvers compared to driving on a straight trajectory. This problem worsens for a decreasing turning radius and an increasing time-gap between the vehicles in the platoon, which results in undesired accelerations in longitudinal direction. Therefore, a solution for this problem during cornering maneuvers needs to be developed to further improve the performance and driving behaviour of vehicle platoons.

The main objective of this thesis is to develop a combined longitudinal and lateral control approach based on the direct vehicle method with an extended look-ahead controller. In the current approaches the length of the path between the vehicles decreases during cornering maneuvers compared to driving on a straight trajectory. The extended look-ahead controller should maintain the inter-vehicle distance independent of whether the vehicle is driving straight or cornering. For this problem during cornering maneuvers a solution needs to be developed and the developed controller needs to be analysed on performance and stability. Vehicle-to-vehicle communication is used to decrease the inter-vehicle distance and increasing the capacity of the roads. A measure for tracking performance needs to be defined to be able to verify the developed controller and to compare the control approach with already existing control approaches. The developed controller needs to be tested through simulations and experiments with the developed controller and the extended look-ahead controller from [1] are performed. This results in the following research objective:

Design an extended look-ahead controller for longitudinal and lateral vehicle tracking which improves tracking performance during cornering maneuvers

This research objective is divided in the following sub-objectives:

- Define a metric that analyses how well the follower vehicle tracks the leader vehicle of the platoon
- Develop a stable longitudinal and lateral controller for cornering maneuvers
- Perform simulations with the developed controller and the already existing controller
- Implement the developed controller in the Renault Twizy to perform experiments with the controller
- Compare tracking performance of the developed controller with the already existing controller

The question that has to be answered is if tracking performance of the developed controller is improved compared to the already existing controller.

1.3 The i-Cave program

This thesis assignment is part of the i-Cave program [9], [10], in this program the focus is on combining cooperative and autonomous driving in a vehicle platform. The vehicle platoon consists of two Renault Twizys, which are modified to be able to perform autonomous and cooperative

driving maneuvers. The modified vehicle can be seen in Figure 1.2. The Renault Twizys are modified to be able to drive both automatically and manually. Inter-vehicle communication is included to be able to improve the collective driving behaviour of the platoon instead of improving single vehicle automated driving.
The i-Cave program consists of seven project groups, which include cooperative vehicle control, communication, human factors and vision. This thesis assignment is part of the cooperative vehicle control project.

Figure 1.2: The modified Renault Twizy that is used in the i-Cave program [9].

1.4 Outline report

This report is organized as follows. Chapter 2 starts with a literature review on longitudinal and lateral vehicle following, which includes the path following method and the direct vehicle following method. In Chapter 3 the extended look-ahead controller approach is discussed and the effective inter-vehicle distance is introduced. A controller is designed to overcome the problem with corner-cutting and the effective inter-vehicle distance. Simulations with the controllers are performed to verify the performance of the controllers. The performance of the controllers is analysed with the developed tracking performance measure. In Chapter 4 the practical set-up with the test vehicles and the implementation of the controllers is discussed. Experiments with the Renault Twizys are performed to further validate the controllers. In Chapter 5 the conclusions and recommendations of this research are given.

Chapter 2

Literature review

2.1 Background

The needs for transportation increases and the effect can be seen in the worldwide vehicle production statistics. Over 39 million cars are manufactured in 1999, this number has increased to 67 million produced passenger cars within 20 years. This is an increase of 28 million produced passenger cars and it is expected that this number grows steadily in the future [11]. This growth in the automobile industry increases the ability of people to access education, employment and other personal needs. However, this development also has some drawbacks, which are traffic congestion, emissions, energy consumption and traffic safety problems.

The traffic congestion problem can be solved by building new infrastructure or by scaling up existing infrastructure. However, due to both financial and environmental reasons this is not always possible. Using the already existing infrastructure could be a solution to increase the road capacity. This can be achieved with some kind of vehicle automation that safely increases the traffic flow [12].
Besides the traffic congestion problem, the traffic emissions are a serious problem where improvements are necessary. The European Commission claims that 50% of the fuel consumption in traffic is caused by congested traffic situations and non-optimal driving behaviour [13]. This suggests that traffic emissions and energy consumption can be decreased when a vehicle automation method, that ensures optimal driving behaviour and an increased traffic flow, is implemented.
Furthermore, 88% of the road accidents with injuries are caused by a human driver [2]. Even when a driver has full focus on the driving task, the human driver will not find the optimal maneuver with respect to safety and fuel efficiency in all cases. The human driver's reaction is based on all accessible information, but in some cases the perception of this information can be limited. This can lead to non-optimal driving maneuvers, which may have great impact on the traffic flow.
A solution for the listed problems is vehicle platooning, this technique is explained in the next section.

2.2 Longitudinal vehicle automation

Vehicle platooning is a technique that can increase the capacity of the already existing roads and highways, while ensuring the traffic safety and decreasing the fuel consumption of a vehicle. The leading vehicle in the platoon is typically driven manually, while for the follower vehicles a part of the driving task is automated. The objective of this system is to maintain a desired inter-vehicle distance $d_{r,i}(t)$ to the preceding vehicle by controlling the propulsive force. The inter-vehicle distance is described as [14]:

$$d_i(t) = x_{i-1}(t) - x_i(t) - L_i \tag{2.1}$$

Here x_i is the position of vehicle i, L_i is the length of vehicle i and i is the indexing of the vehicles. The spacing error is formulated as [14]:

$$e_i(t) = d_i(t) - d_{r,i}(t) \tag{2.2}$$

In Figure 2.1 the desired inter-vehicle distance, the actual inter-vehicle distance and the spacing error in longitudinal vehicle platooning are depicted. In longitudinal vehicle platooning it is important to minimize the spacing error, where the reference for the inter-vehicle distance is obtained from spacing policies, which are discussed in the next subsection.

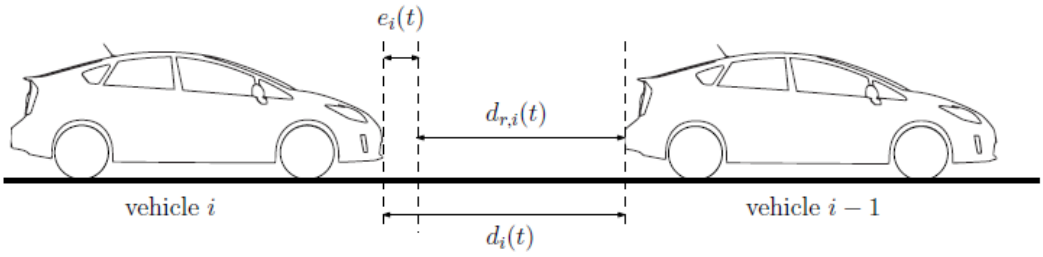

Figure 2.1: The desired inter-vehicle distance $d_{r,i}$, the actual inter-vehicle distance d_i and the spacing error e_i in longitudinal vehicle platooning [1].

2.2.1 Spacing policies

In longitudinal vehicle platooning the controller tries to maintain the desired inter-vehicle distance $d_{r,i}(t)$ by minimizing the spacing error $e_i(t)$. For the automation of the longitudinal motion of the vehicle different inter-vehicle distances can be used, these distances are obtained from spacing policies. In literature the following spacing policies are discussed: the constant distance policy [15], [16], [17], the constant time-gap policy [14], [18] and the varying time-gap policy [19], [20].

The simplest spacing policy is the constant distance policy. In this policy the inter-vehicle distance is constant and independent of the vehicle speed. This means that the inter-vehicle distance at a highway is the same as the distance at low speeds.

In the constant time-gap policy the inter-vehicle distance linearly depends on the follower vehicle's velocity. This means that the inter-vehicle distance is smaller at low speeds than at high speeds, this is defined as:

$$d_{r,i}(t) = r_i + h_i v_i(t) \tag{2.3}$$

Here r_i is the standstill distance, h_i is the desired time-gap and $v_i(t)$ is the velocity of vehicle i. The constant time-gap spacing policy is safer compared to the constant distance spacing policy, since the inter-vehicle distance increases for increasing speeds.

Another option is the varying time-gap policy, in this spacing policy the time-gap depends on the relative velocity between the follower vehicle and the preceding vehicle. The varying time-gap policy is defined as:

$$d_{r,i}(t) = r_i + h_i(t) v_i(t) \tag{2.4}$$

Here the time-gap $h_i(t)$ depends on the relative velocity between the follower vehicle and the preceding vehicle, which can be written as:

$$h_i(t) = h_{0,i} - c_i v_{r,i}(t) \tag{2.5}$$

Where $h_{0,i}$ and c_i are constants and $v_{r,i}(t) = v_{i-1}(t) - v_i(t)$. With this policy the follower vehicle reduces the time-gap when the preceding vehicle is moving faster than the follower vehicle to

decrease the inter-vehicle distance and increase the traffic throughput.

The different spacing policies have impact on the string stability of the vehicle platoon. In the following subsection longitudinal string stability is explained.

2.2.2 Longitudinal string stability

The term string stability is introduced during the development of vehicle platooning. String stability is the capability of a vehicle platoon in attenuating disturbances or errors introduced by any vehicle in the platoon [14]. These disturbances or errors can be speed variations or positions errors between vehicles. A platoon is considered string stable if any disturbance or error in the vehicle platoon with respect to the desired signal attenuates towards the tail of the platoon.
An example can be seen in Figure 2.2. Here a platoon consisting of 4 vehicles is depicted and x_i denotes the position error of vehicle i at time t. It can be seen that in the case where the platoon is string unstable (Figure 2.2(b)) the position errors are amplified along the vehicle string, while in the case where the platoon is string stable 2.2(c)) the position errors are attenuated along the string.

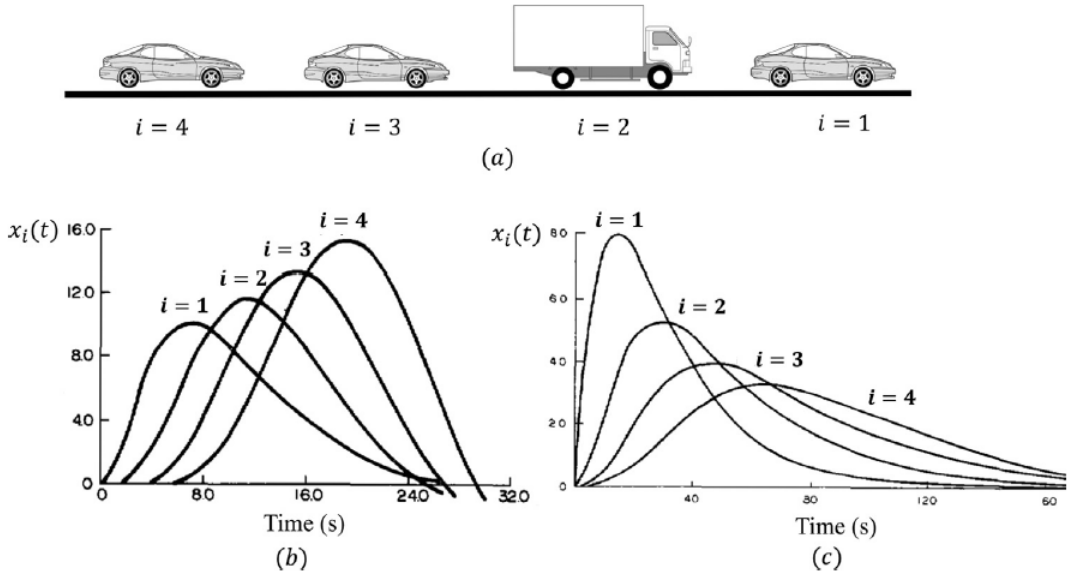

Figure 2.2: String stability of a vehicle platoon [21].

In [14] a definition for longitudinal string stability of vehicle platoons is proposed. Here the following interconnected system is considered:

$$\mathcal{S}\begin{cases} \dot{x}_i = f_i\left(x_i, x_{i-1}, \ldots, x_2, x_1, u_1\right) \\ y_i = h\left(x_i\right), \quad i = 1, 2, \ldots, m, \text{ with } m \in \mathbb{N} \end{cases} \tag{2.6}$$

The input-output behaviour in the Laplace-domain of the system S is defined as:

$$y_i(s) = P_i(s)u_1(s), \quad i = 1, \ldots, m, \text{ with } m \in \mathbb{N} \tag{2.7}$$

With the string stability complementary sensitivity:

$$\Gamma_i(s) = P_i(s)P_{i-1}^{-1}(s), \quad i \geq 2 \tag{2.8}$$

$\mathcal{L}_2$ string stability means that the energy of the output error is smaller than the energy of the input error, but this does not mean that the spacing error attenuates along the vehicle string. The system S is strictly $\mathcal{L}_2$ string stable in the longitudinal direction of the vehicle if the following conditions hold: [14]

1) $\|P_1(j\omega)\|_{\mathcal{H}_\infty}$ exists
2) $\|\Gamma_i(j\omega)\|_{\mathcal{H}_\infty} \leq 1, \forall i \in \mathbb{N}\backslash\{1\}$

$\mathcal{L}_\infty$ string stability means that maximum magnitude of the output error is smaller than the input error, this means that spacing errors attenuates along the vehicle string. The system S is strictly $\mathcal{L}_\infty$ string stable in the longitudinal direction of the vehicle if the following conditions hold: [14]

1) $\|p_1(t)\|_{\mathcal{L}_1}$ exists
2) $\|\gamma_i(t)\|_{\mathcal{L}_1} \leq 1, \quad \forall i \in \mathbb{N}\backslash\{1\}$

Here $p_1(t)$ and $\gamma_i(t)$ are the impulse responses corresponding to $P_1(s)$ and $\Gamma_i(s)$ respectively, it is assumed that P_i^{-1} exists for all i.

Besides automation in the longitudinal direction of the vehicle, automation in the lateral direction of the vehicle is an option in vehicle platooning. The concept of lateral vehicle automation is discussed in the next section.

2.3 Lateral vehicle automation

Lateral vehicle automation is a technique that is used to increase ride comfort and safety. Lateral vehicle automation, which is also known as automatic steering, is a form of automation that keeps the vehicle in the lane center or that follows a preceding vehicle in lateral sense. Compared to longitudinal vehicle automation, the lateral control objective can be defined in many ways such as: [22]

- At the vehicle's center of mass
- At a look-ahead distance
- At the center of the rear bumper of the preceding vehicle

These different lateral control objectives are depicted in Figure 2.3. Various examples of lateral vehicle automation with the described control objectives can be found in literature and these are discussed in this section.

In [23], [24], [25] and [26] the look-down sensing approach is used, where magnetic markers are embedded in the center of the lane and the vehicles are equipped with a magnetometer. These magnetic markers are used for the lateral controller to let the vehicle's center of mass track the center of the lane. This technique is further explained in Section 2.4, where longitudinal and lateral vehicle automation are combined.

In [27] the lateral control problem for lane-keeping in a highway environment is discussed. In this research the look-ahead approach is used, since with this approach the already existing infrastructure can be used. The vehicle's lateral dynamics are described by the single track vehicle model, this simple model provides a sufficient accurate description of the lateral vehicle dynamics under certain conditions. These conditions are for example that the vehicle has to drive on a flat road with large radii corners at a relative constant velocity, which is the case in a highway environment. In this research a vision-system is installed on a Fiat Brava. The vision-system consists of a video-camera that is positioned at the wind shield of the vehicle and an image processing algorithm that

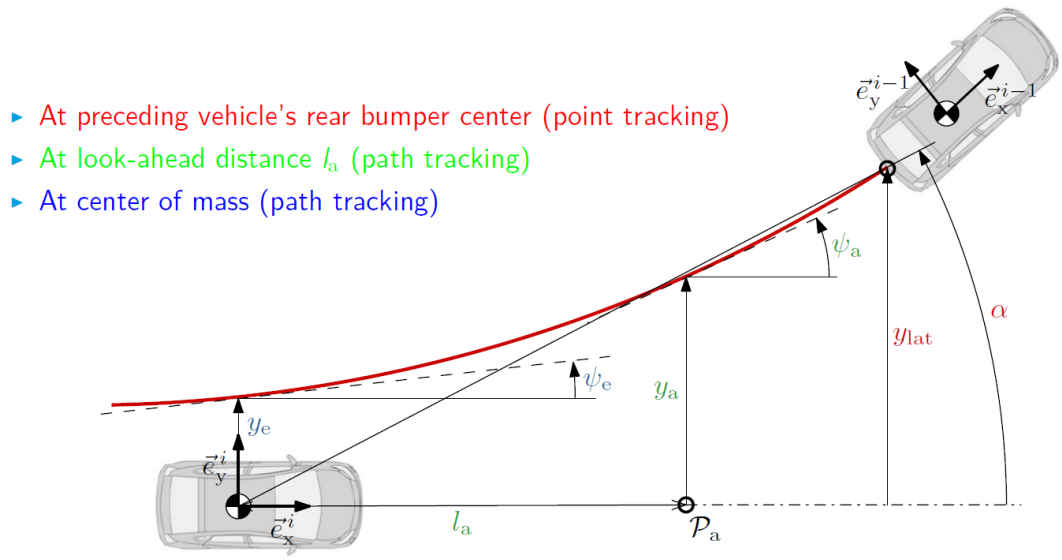

Figure 2.3: The different lateral control objectives [22].

provides the relevant information about the position of the vehicle on the road. The vision-system provides the value of the parameters m and q, which can be seen in Figure 2.4. Here m is the angle between linear approximation of the center-line of the lane and the longitudinal axis of the vehicle, while q is the distance along the y-axis between the linear approximation of the center-line of the lane and the center of gravity of the vehicle. The look-ahead distance L of the vehicle has a value between 3 and 20 meters. With these quantities the feedback output approximation y_{fb} can be calculated, which is the distance measured at the look-ahead point between the longitudinal axis of the vehicle and the linear approximation of the center-line of the lane. Two controllers are designed, where one controller is designed to obtain better lane-keeping, while the other controller is designed to optimize ride comfort. These two controllers are designed in order to make a trade-off between lane-keeping and ride comfort. Experiments with both controllers are performed at a highway with a turning radius of 1000 m with a constant velocity of 100 km/h. Results show that the position error with respect to the center-line of the lane is kept below the specified 20 cm. The controller that is optimized for ride comfort leads to a more comfortable ride according to the test-drivers, which also is confirmed by the experimental data.

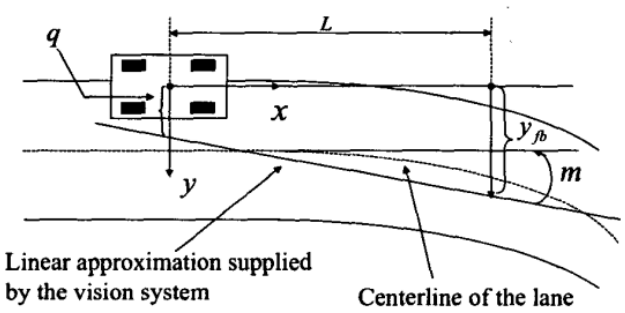

Figure 2.4: The approximation of the center of the lane provided by the vision-system [27].

Subsequently, the controller developed in [27] is used in [28] to combine automatic lane-keeping

and the ability for a drivers' steering intervention in order to avoid obstacles or to change lanes. A control scheme is developed where the vehicle center of gravity tracks the center-line of the lane when there is no steering intervention from the driver. When there is steering action from the driver, the vehicle lateral dynamics are fully controlled by the driver. Simulations and experiments on highways with a Fiat Brava show that the controller keeps the vehicle at the center-line of the lane when there is no steering input from the driver. When the driver applies a torque on the steer, the lane-keeping task is released by the controller and from that moment the driver has full control to perform a lane change. At the end of the maneuver the controller resumes smoothly with the lane-keeping task.

In recent years this technique is further developed, where camera and post-processing is used to yield third or fifth order polynomials to obtain the lane center-line polynomial. In [29] a robust multi-rate lane-keeping control scheme is developed. In this research a controller is developed and implemented in a Hyundai Tucson equipped with a vision system, a yaw-rate sensor and a wheel speed sensor. A linear quadratic state feedback controller is developed that uses the lateral offset at the look-ahead distance. The system is called a multi-rate system, since the camera from the vision system has a slower update-rate than the other sensors. To address this problem a multi-rate Kalman filter is developed, this filter estimates the vehicle state by using the measured data from the camera at a fast rate. These estimated states are used by the developed linear quadratic state feedback controller to improve lane-keeping performance. A third order polynomial from the left and the right lane is defined by using the data obtained from the camera. The average of these polynomials is taken to obtain the desired lane polynomial. This predicted virtual lane can be used when the camera has a temporary failure, thus the developed controller can normally operate when lane information is temporarily unavailable. Experiments are performed at a circuit and results show that lateral vehicle automation is successfully implemented. The developed controller operates normally with the predicted virtual lane when lane information is temporarily unavailable.

In the previous sections longitudinal and lateral vehicle automation are discussed separately. These techniques can be combined to obtain combined longitudinal and lateral vehicle automation and this is discussed in the following section.

2.4 Combined longitudinal and lateral vehicle automation

For combined longitudinal and lateral vehicle automation the concepts of separate longitudinal and lateral automation can be utilized. For this form of automation two methods are considered, which are path following and direct vehicle following. The path following method follows a predefined path, while the direct vehicle method tracks and follows a preceding vehicle, these concepts are elaborated in the next subsections.

2.4.1 Path following

In the path following method the vehicle follows a predefined path and to be able to do this the positions and curvature of this path at any point are needed. This path can be created from road marking or from the path of a preceding vehicle. The path following method is used in literature repeatedly, below a number of implementations are discussed.

In [5] it is shown that a platoon consisting of eight vehicles is able to drive at a short inter-vehicle distance. The longitudinal and the lateral controller are developed separately and thus longitudinal spacing control and lateral lane changing can be executed separately. The center-lines of the highway are equipped with magnetic markers in this research, these magnetic markers are for the lateral controller. Experiments with the controller with velocities up to 130 km/h show that the vehicles in the platoon are able to travel with an inter-vehicle distance of 6.5 m with a maximum spacing error of 0.2 m and lateral lane changing is possible with an accuracy of 0.1

m. The following maneuvers are possible with the developed controller: starting from standstill, accelerating to the desired velocity and subsequently maintaining this desired velocity, automatic steering for lane-keeping and lane-changing, allowing new vehicles to enter the platoon and stopping the platoon at the end of the road. The drawback of this system is that all roads need to be embedded with magnetic markers.

In [6] an RTK-GPS (Real Time Kinematic Global Positioning System) is used to measure the position of the vehicles in the platoon. With this system the position of the vehicles can be determined within 1 cm accuracy. Vehicle-to-vehicle communication via Wi-Fi is used to share the absolute position measurements with the other vehicles. Longitudinal and lateral control are fully decoupled by using nonlinear techniques. The constant distance spacing policy is used for the longitudinal controller, while the path following technique is used for the lateral controller. For the experiments a platoon consisting of two vehicles is used, where the lateral error is maintained with an accuracy of 2 cm. For longitudinal control the inter-vehicle distance is maintained with a standard deviation of 4.7 cm and the mean error is 1 cm. The drawback of this system is that the RTK-GPS is very expensive and as a result commercial vehicles are not equipped with this system.

2.4.2 Direct vehicle following

The goal of vehicle platooning is to let the vehicles in the platoon drive at a short inter-vehicle distance to increase the road capacity. But when the vehicles in the platoon are driving close to each other the camera cannot track the road markings and thus the path following approach does not work. A solution for this problem is the direct vehicle following method, since this technique does fully operate in cases where road markings or lane information are not available. For this technique path information is not needed, since this approach tracks the location and heading angle of the preceding vehicle. The preceding vehicle's current relative position can be measured by the radar, while velocity and acceleration can by communicated through vehicle-to-vehicle communication.

The direct vehicle approach utilizes the already available information from CACC, therefore this method is more cost-effective than the path following method. However, when using this approach the follower vehicle may cut corners [1]. A problem arises when the controller senses a difference in the orientation between the follower vehicle and the preceding vehicle. In this case the controller may command the preceding vehicle to turn too early and this results in corner-cutting behaviour. This corner-cutting behaviour can be compensated and several strategies are proposed in literature. These methods are using a virtual reference point linked with the rear of the preceding vehicle and this virtual reference point acts as the reference point for the follower vehicle. When the follower vehicle follows the virtual reference point, the corner cutting is compensated [1].

In [8] the follower vehicle follows the leader vehicle without using information about the road infrastructure or vehicle-to-vehicle communication. The follower vehicle only uses information from on-board sensors such as the current relative position and orientation with respect to the preceding vehicle. In this research it is assumed that the preceding vehicle's velocity and angular velocity are not known by the follower vehicle, but are constant parameters and that the curvature of the path of the preceding vehicle is also not known. A controller is designed for the follower vehicle which tracks the path taken by the preceding vehicle, at steady-state, with a prescribed inter-vehicle distance. The follower vehicle tracks a virtual reference point, this point is located at a known and desired distance behind the preceding vehicle instead of tracking the rear of this vehicle to compensate for corner-cutting behaviour. The virtual reference point can be seen in Figure 2.5. Here R_{1r} is the virtual reference point associated with the lead vehicle and R_{2f} is the virtual reference point of the following vehicle. Simulations with a two degrees of freedom bicycle model are performed. In these simulations the platoon consists of two vehicles and the preceding vehicle's path consists of three consecutive maneuvers performed at constant velocities:

turning to the left, turning to the right and then a straight line motion. Results show that with this approach the problem of corner-cutting is solved, since the follower vehicle successfully tracks the path taken by the preceding vehicle.

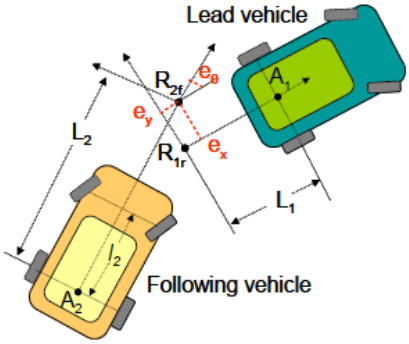

Figure 2.5: The virtual reference point to avoid corner-cutting [8].

In [30] a control algorithm is developed that controls both the longitudinal and the lateral dynamics of the vehicles in the platoon. This algorithm uses the information provided by the on-board sensors and the preceding vehicle's states, which are communicated via vehicle-to-vehicle communication. The follower vehicle tracks the preceding vehicle at a certain distance ahead its own center of gravity and this distance is called the look-ahead distance. In this research it is assumed that all vehicles drive with a constant velocity and that the vehicle parameters are known for all vehicles in the platoon. A platoon that consists of 17 vehicles is simulated, where the platoon is driving on a straight road and a lateral disturbance is applied on the second vehicle of the platoon. This disturbance is applied to observe if this error will propagate in the platoon. Results show that the error in the platoon attenuates and even reaches zero.

In this section the direct vehicle method is discussed, here a controller that uses a look-ahead distance to track the preceding vehicle is introduced. In the next section the look-ahead controller developed in [1] is explained, since this controller is used as a starting point for the controller developed in this research.

2.5 Conventional look-ahead controllers

In literature several controllers that are based on the look-ahead approach are developed, an example can be found in [1]. Where the objective of the controller is to follow the preceding vehicle at a desired distance. The constant time-gap spacing policy is used to describe this desired distance, so the desired inter-vehicle distance is $d_{r,i} = r_i + h_i v_i$. However, in this research the desired spacing distance is defined as a vector, which is seen as a look-ahead in the direction of the heading angle θ_i with respect to the global x-axis of the follower vehicle. This look-ahead distance is depicted in Figure 2.6. The spacing error e_i is defined as the difference between the desired inter-vehicle distance $d_{r,i}$ and the actual inter-vehicle distance d_i as can be seen in the figure. A controller is designed that minimizes this spacing error and simulations and experiments with this controller are performed. Results show that this controller performs well on a straight path, the vehicles drive at the desired inter-vehicle distance without a lateral error. However, when the platoon enters a circular path the controller has its shortcomings. The follower vehicles in the platoon are cruising with a smaller turning radius than their preceding vehicle, this is known as corner-cutting. This behaviour occurs because when the preceding starts cornering, the follower

vehicle detects a spacing error. The controller reacts instantaneously and adjusts the position of the follower vehicle to minimize the error, which leads to corner-cutting. Since the follower vehicles drive in a smaller radius, the velocity of the follower vehicles is lower than the preceding vehicle and this affects the spacing policy.

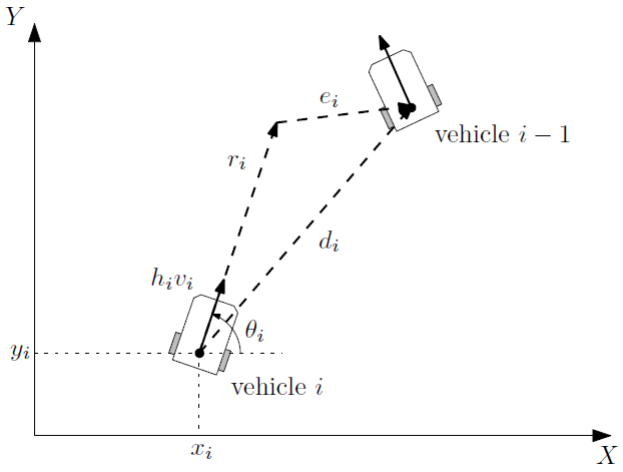

Figure 2.6: Look-ahead of the follower vehicle with spacing error e_i and the actual distance d_i between vehicle i and $i-1$ [1].

To prove that the look-ahead controller from [1] cuts corners, this controller is implemented in Matlab and simulations are performed. For the simulations a platoon consisting of 3 vehicles is chosen. In Figure 2.7 the trajectories of the vehicles in the platoon can be seen. From this figure it becomes clear that the follower vehicles are driving with a smaller turning radius than their preceding vehicle, thus corner-cutting behaviour is observed.

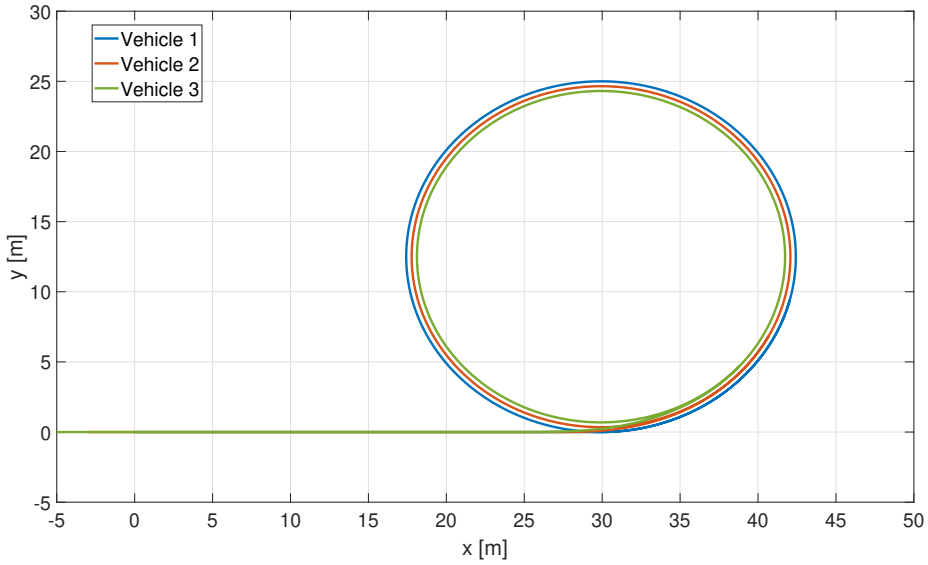

Figure 2.7: The trajectory of the vehicles in the platoon.

2.6 Conclusions

In this chapter the relevant literature and developments in vehicle platooning are discussed. First, the background of vehicle platooning is discussed. This shows the problems of the growth in the automobile industry, the proposed solution for these problems is vehicle platooning. The concept of longitudinal vehicle automation is explained with the corresponding spacing policies. The different spacing policies have impact on string stability, so subsequently longitudinal string stability is discussed. After that lateral vehicle automation is elaborated, where it is seen that the lateral control objective can be defined in many ways. Next, combined longitudinal and lateral vehicle automation is introduced. For this higher level of automation two methods are discussed: path following and direct vehicle following. For the path following method the infrastructure needs to be adapted or all vehicles need to be equipped with the expensive RTK-GPS. The direct vehicle follower method utilizes the already available information from CACC and does not need lane information or lane markings. In literature several controllers that are based on the direct vehicle method are discussed. However, simulations and experiments with the look-ahead controller show that this controller tends to cut corners. A solution for the corner-cutting behaviour with look-ahead controllers is discussed in the next chapter.

Chapter 3

Extended look-ahead controller

From the previous chapter we know that with conventional look-ahead controllers corner-cutting behaviour is observed. An extended look-ahead controller is developed in [1], which compensates for the corner-cutting behaviour, while maintaining a safe inter-vehicle distance. However, a variation in the inter-vehicle distance is seen with this controller as becomes clear later in this chapter. First, the extended look-ahead controller is discussed in this section to fully understand the cause of this variation in inter-vehicle distance. After that, the variation in inter-vehicle distance is shown with simulations and then a controller that solves this problem is developed. For validation, simulations with the extended look-ahead controller and the developed controller are performed. In the last section the conclusions of this chapter are summarized.

3.1 Extended look-ahead controller design

For the extended look-ahead approach from [1] the vehicles in the platoon are modelled as unicycles on a Cartesian coordinate system, this vehicle model is described by the following equations:

$$\dot{x}_i(t) = v_i(t)\cos\theta_i(t) \tag{3.1}$$

$$\dot{y}_i(t) = v_i(t)\sin\theta_i(t) \tag{3.2}$$

$$\dot{v}_i(t) = a_i(t) \tag{3.3}$$

$$\dot{\theta}_i(t) = \omega_i(t) \tag{3.4}$$

Here x_i and y_i are the unicycle's Cartesian coordinates, θ_i is the heading angle of the unicycle with respect to the global x-axis, v_i is the longitudinal velocity of the unicycle, a_i is the longitudinal acceleration input and ω_i is the angular velocity input. The unicycle on the Cartesian coordinate system is depicted in Figure 3.1. The indexing of the unicycles is described with i, which is increasing in the upstream direction of the platoon. From this point the time argument t is omitted in this report for readability.

The objective of this system is to maintain a desired inter-vehicle distance $d_{r,i}$ to the preceding vehicle by controlling the acceleration of the vehicles in the platoon. For this controller design the constant time-gap policy is chosen, this spacing policy is defined as:

$$d_{r,i} = \begin{bmatrix} d_{rx,i} \\ d_{ry,i} \end{bmatrix} = (r_i + h_i v_i) \begin{bmatrix} \cos\theta_i \\ \sin\theta_i \end{bmatrix} \tag{3.5}$$

Here r_i is the standstill distance and h_i is the desired constant time-gap. The spacing distance is formulated as a vector with angle θ_i with respect to the global x-axis, which can be seen as a look-ahead distance in the direction of the orientation of the vehicle, this is shown in Figure 2.6.

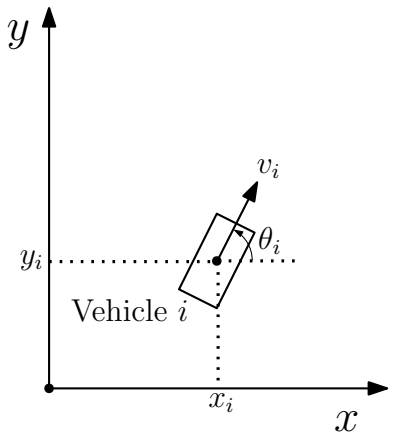

Figure 3.1: Unicycle on a Cartesian coordinate system.

With a conventional look-ahead controller the follower vehicle's lateral error is only zero when the platoon is driving on a straight line [1]. When the preceding vehicle starts cornering, the follower vehicle senses a position error due to the look-ahead strategy. To correct errors the follower vehicle starts cornering sooner instead of waiting until it arrives at the actual point of the corner, this problem is known as corner-cutting.

This problem can be solved by extending the look-ahead point of vehicle i, which creates a "virtual" vehicle that acts as a reference for the follower vehicle i. Thus the look-ahead point of vehicle i is extended and with the extended look-ahead vector, vehicle i follows the virtual vehicle attached to vehicle $i-1$ to let vehicle i turn at the actual point of the corner and to correct for the unintended lateral error.

The extended look-ahead point of which the coordinates are defined as $s_{i-1} = [s_{x,i-1}, s_{y,i-1}]^T$, extends perpendicular from the heading direction of vehicle $i-1$ and can be used as a reference tracking point for vehicle i, this can be seen in Figure 3.2. The spacing error of the extended look-ahead design is formulated as:

$$e_i = (p_{i-1} + s_{i-1}) - (p_i + r_i + h_i v_i) \tag{3.6}$$

Here $p_i = [x_i, y_i]^T$ is the position of vehicle i. The look-ahead point s_{i-1} can be written in Cartesian coordinates as:

$$s_{x,i-1} = \bar{s}_{i-1} \sin\theta_{i-1} \tag{3.7}$$

$$s_{y,i-1} = -\bar{s}_{i-1} \cos\theta_{i-1} \tag{3.8}$$

Here $\bar{s}_{i-1}$ is the magnitude of s_{i-1}. The magnitude of the extension vector needs to be determined such that all vehicles in the platoon turn with the same turning radius. Because this extension vector always extends perpendicular to the heading direction of vehicle $i-1$, only the extension vector's magnitude has to be calculated.

In [1] an expression for the magnitude of the extension vector $\bar{s}_{i-1}$ is derived by analyzing the behaviour of the platoon when this platoon is driving steady-state in a circular movement. The assumption is made that the heading angle difference between the vehicles is not bigger than $\pi/2$ in order to make sure that the extension vector can always be defined. In Figure 3.3 it can be seen that vehicle $i-1$ turns towards the positive y-axis. In steady-state vehicle $i-1$ has a turning radius R_{i-1} and the tracking point of vehicle i is extended to point S. By using the Pythagorean theorem it follows that:

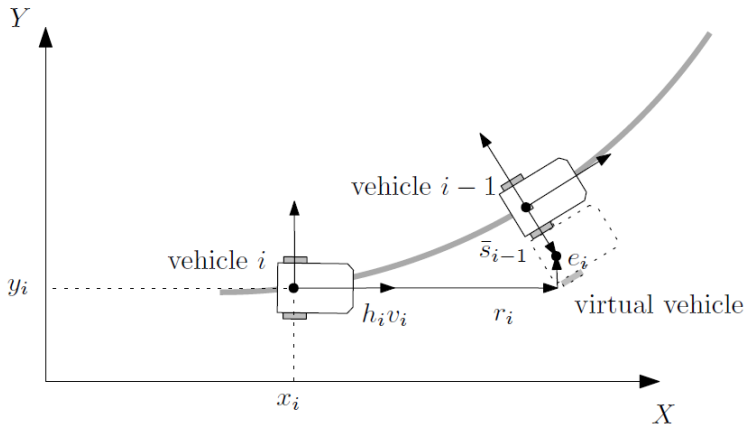

Figure 3.2: The extended look-ahead approach with the virtual vehicle and spacing error e_i [1].

$$(R_{i-1} + \bar{s}_{i-1})^2 = R_{i-1}^2 + (r_i + h_i v_i)^2 \tag{3.9}$$

The path curvature κ_{i-1} can be calculated with the following equation:

$$\kappa_{i-1} = \frac{1}{R_{i-1}} = \frac{\omega_{i-1}}{v_{i-1}} \tag{3.10}$$

This means that κ_{i-1} is zero when vehicle $i-1$ is not cornering, thus in that case the magnitude of the extension vector should be zero. By rearranging (3.9) and taking into account that the magnitude of the extension vector should be zero when the leader vehicle is not cornering, the magnitude of the extension vector can be formulated as:

$$\bar{s}_{i-1} = \begin{cases} 0 & \text{for } \kappa_{i-1} = 0 \\ \frac{-1+\sqrt{1+\kappa_{i-1}^2 (r_i + h_i v_i)^2}}{\kappa_{i-1}} & \text{for } \kappa_{i-1} \neq 0 \end{cases} \tag{3.11}$$

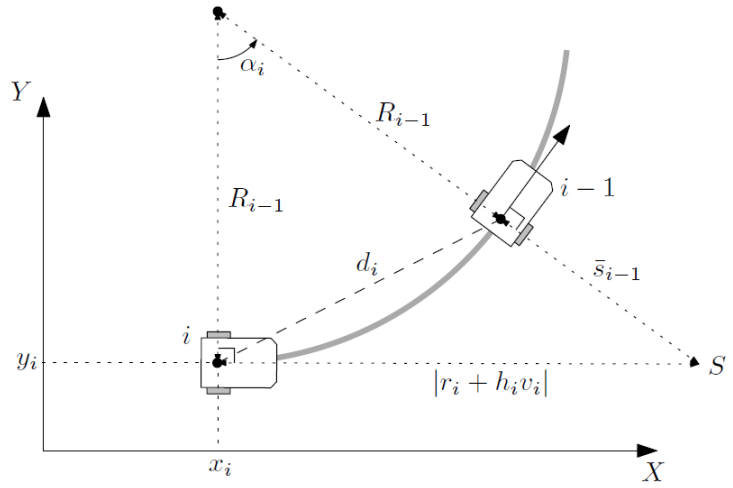

Figure 3.3: Magnitude of the extension vector $\bar{s}_{i-1}$ [1].

The state components are derived for the extended look-ahead approach. The position errors in x- and y-direction are used as state components $z_{1,i}$ and $z_{2,i}$, while $z_{3,i}$ and $z_{4,i}$ are the velocity errors of the vehicle in x- and y-direction respectively:

$$z_{1,i} = x_{i-1} + s_{x,i-1} - x_i - (r_i + h_i v_i)\cos\theta_i \tag{3.12}$$

$$z_{2,i} = y_{i-1} + s_{y,i-1} - y_i - (r_i + h_i v_i)\sin\theta_i \tag{3.13}$$

$$z_{3,i} = v_{i-1}\cos\theta_{i-1} - v_i\cos(\theta_i + \alpha_i) \tag{3.14}$$

$$z_{4,i} = v_{i-1}\sin\theta_{i-1} - v_i\sin(\theta_i + \alpha_i) \tag{3.15}$$

Here α_i is the angle of arc between vehicle i and vehicle $i-1$. This angle of arc is included to $z_{3,i}$ and $z_{4,i}$ to guarantee that $z_{3,i}$ and $z_{4,i}$ converge to zero independent of whether the vehicle is driving on a straight trajectory or on a curved trajectory. The angle of arc α_i can be derived from Figure 3.3 and can be written as:

$$\alpha_i = \arctan\left[\kappa_{i-1}(r_i + h_i v_i)\right], \quad -\frac{\pi}{2} < \alpha_i < \frac{\pi}{2} \tag{3.16}$$

A controller input $[a_i, \omega_i]^T$ is designed in [1] which asymptotically stabilizes this system at zero, this controller input is defined as:

$$\begin{bmatrix} a_i \\ \omega_i \end{bmatrix} = \Gamma_{12,i}^{-1}\left(\begin{bmatrix} k_1 z_{1,i} \\ k_2 z_{2,i} \end{bmatrix} + \frac{1}{\cos\alpha_i}\begin{bmatrix} z_{3,i} \\ z_{4,i} \end{bmatrix} + \beta_{1,i}\right) \tag{3.17}$$

Where

$$\Gamma_{12,i}^{-1} = \frac{1}{\mu_i}\begin{bmatrix} (r_i + h_i v_i)\cos\theta_i & (r_i + h_i v_i)\sin\theta_i \\ -h_i\sin\theta_i - s_{a,i}\cos\theta_{i-1} & h_i\cos\theta_i - s_{a,i}\sin\theta_{i-1} \end{bmatrix} \tag{3.18}$$

$$\mu_i = h_i(r_i + h_i v_i)(1 - \sin\alpha_i\sin(\theta_{i-1} - \theta_i)) \tag{3.19}$$

$$\begin{aligned} \beta_{1,i} = {} & \begin{bmatrix} -\sin\theta_i \\ \cos\theta_i \end{bmatrix} v_i\tan\alpha_i + R(\theta_{i-1})\begin{bmatrix} \bar{s}_{i-1}\omega_{i-1} \\ -s_{\kappa,i}\dot{\kappa}_{i-1} \end{bmatrix} \\ & + \left(1 - \frac{1}{\cos\alpha_i}\right)\begin{bmatrix} \cos\theta_{i-1} \\ \sin\theta_{i-1} \end{bmatrix} v_{i-1} \end{aligned} \tag{3.20}$$

$$R(\theta_{i-1}) = \begin{bmatrix} \cos\theta_{i-1} & -\sin\theta_{i-1} \\ \sin\theta_{i-1} & \cos\theta_{i-1} \end{bmatrix} \tag{3.21}$$

$$s_{a,i} := h_i\sin\alpha_i \tag{3.22}$$

$$s_{\kappa,i} := \frac{1}{\kappa_{i-1}^2}(1 - \cos\alpha_i) \tag{3.23}$$

3.2 Effective inter-vehicle distance

The extended look-ahead controller from [1] as described in the previous section successfully compensates for corner-cutting behaviour as becomes clear later in this chapter. However, with this extended look-ahead controller another problem arises. When the platoon is driving on a straight line the desired inter-vehicle distance, $d_{r,i} = r_i + h_i v_i$, equals the actual length of the path between vehicle i and vehicle $i-1$. On the other hand, during cornering the actual length of the path between vehicle i and vehicle $i-1$ does not equal the desired inter-vehicle distance, $d_{r,i} = r_i + h_i v_i$. In this section it is shown that the actual length of the path between the vehicles is shorter for cornering maneuvers compared to driving on a straight line. This results in undesired accelerations in longitudinal direction when the platoon enters a circular movement after driving straight.

This is caused by the method by which the extended look-ahead point is defined. When the platoon starts cornering, the look-ahead point of vehicle i is extended. This creates a virtual vehicle that acts as a new tracking objective for vehicle i. With equation (3.11) the magnitude of the extension vector $\bar{s}_{i-1}$ can be determined such that the corner-cutting behaviour of the vehicles in the platoon is prevented. This extended look-ahead point S, as can be seen in Figure 3.3, is considered as the new tracking point objective of vehicle i. In other words, when vehicle $i-1$ starts cornering the tracking point objective of vehicle i shifts from the base of vehicle $i-1$ to the extended look-ahead point S.
The problem is that the controller maintains the distance from the base of vehicle i to the extended look-ahead point S equal to $r_i + h_i v_i$. However, the controller should maintain the actual length of the path between vehicle i and vehicle $i-1$ equal to $r_i + h_i v_i$, while still compensating for the corner-cutting behaviour. The actual length of the path between vehicle i and vehicle $i-1$ is called the effective inter-vehicle distance from here. From Figure 3.3 it can be seen that the effective inter-vehicle distance does not equal the desired inter-vehicle distance $d_{r,i} = r_i + h_i v_i$.

Figure 3.4 shows the effective inter-vehicle distance, which is calculated as the path length between vehicle i and vehicle $i-1$. Here the path length is calculated as the product of the angle of arc α_i and the turning radius R_{i-1}. From the figure it can be seen that the effective inter-vehicle distance decreases for a decreasing turning radius of vehicle $i-1$ for different time-gaps with the extended look-ahead controller from [1]. Here the standstill distance $r_i = 1$ m and the velocity $v_i = 5$ m/s are arbitrarily chosen. The solid lines represent the effective inter-vehicle distances with the extended look-ahead controller from [1] and the dotted lines represent the desired spacing distance $d_{r,i} = r_i + h_i v_i$ according to the constant time-gap spacing policy.
From the figure it becomes clear that the effective inter-vehicle distance does not equal the desired inter-vehicle distance as prescribed by the chosen spacing policy when the extended look-ahead controller from [1] is applied. The dotted lines represent the desired inter-vehicle distances and these distances are independent of the turning radius R_{i-1}. It can be seen that the effective inter-vehicle distance decreases for a decreasing turning radius and this problem worsens for bigger time-gaps. With a time-gap of $h_i = 2$ s the inter-vehicle distance is affected the most, the desired inter-vehicle distance is 11 m, while the effective inter-vehicle decreases to 4.3 m for the minimum turning radius, which is a decrease of 60.6%. For a time-gap of $h_i = 1$ s the desired inter-vehicle distance equals 6 m, while the effective inter-vehicle decreases with 40.2% to 3.6 m for the minimum turning radius. For the time-gaps $h_i = 0.5$ s and $h_i = 0.25$ s the desired inter-vehicle distances are 3.5 m and 2.25 respectively, while the effective inter-vehicle distances decrease with 22.3% and 11.6% to 2.72 m and 1.99 m respectively.

So, when the platoon is driving on a straight trajectory the effective inter-vehicle distance is equal to the desired inter-vehicle distance. But when then the platoon is cornering the effective inter-vehicle distance is not equal to the desired inter-vehicle distance and this problem worsens for a decreasing turning radius and an increasing time-gap. Deceasing the effective inter-vehicle distance during cornering can be seen as undesired behaviour, since this leads to undesired accelerations in longitudinal direction. The extended look-ahead controller should maintain the effective inter-vehicle distance at $r_i + h_i v_i$ independent of whether the vehicle is driving straight or cornering.

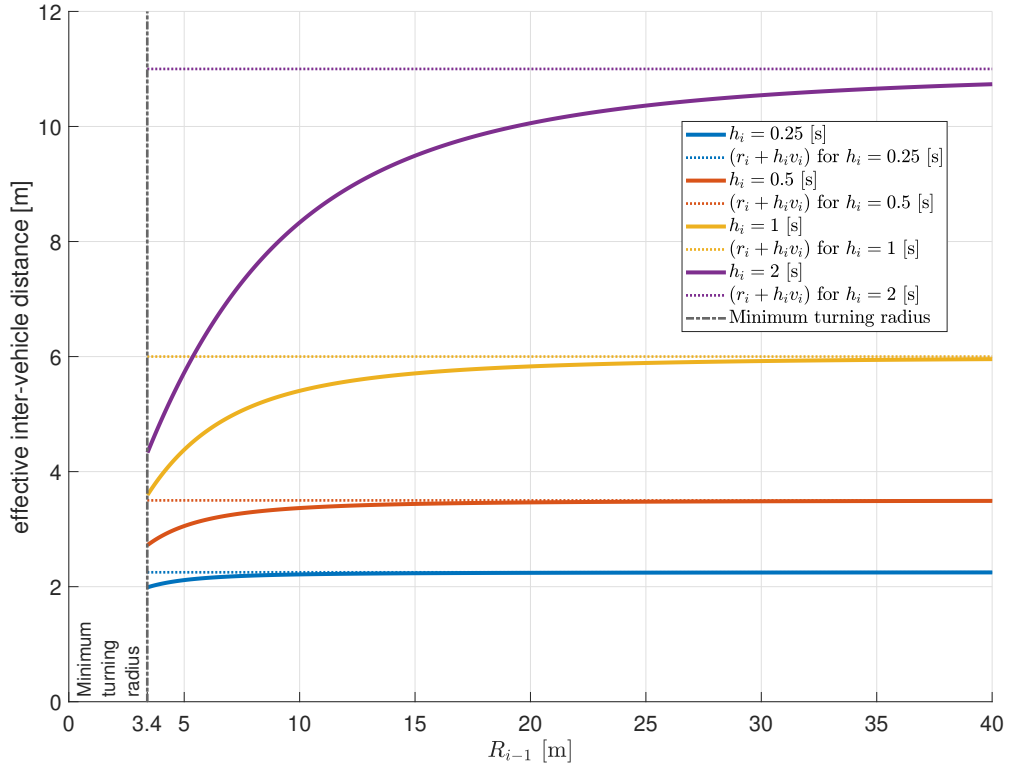

Figure 3.4: The effective inter-vehicle distance as a function of the turning radius R_{i-1} for variable time-gaps with $r_i = 1$ [m] and $v_i = 5$ [m/s].

3.3 Vehicle following controller with extended look-ahead

In the previous section the importance of maintaining the effective inter-vehicle distance while driving on a straight line and while cornering is shown. Therefore, an extended look-ahead controller that compensates for corner-cutting behaviour and that maintains the effective inter-vehicle distance at $r_i + h_i v_i$ independent of whether the vehicle is driving straight or cornering is developed in this section. The extended look-ahead controller from [1] is used as a base for the controller, since this extended look-ahead controller successfully compensates for corner-cutting behaviour of vehicles in the platoon.

The vehicles in the platoon are modelled as unicycles on a Cartesian coordinate system as can be seen in equations (3.1-3.4). The objective of the controller is to maintain the effective inter-vehicle distance $d_{r,i}$ to the preceding vehicle by controlling the acceleration of the vehicles in the platoon, independent of whether the vehicle is driving straight or cornering. The constant time-gap spacing policy from [14], as can be seen in equation (3.5), is chosen for this controller.

The other objective of the controller is to compensate for the corner-cutting behaviour that is seen with conventional look-ahead controllers. To compensate for this corner-cutting behaviour a "virtual" vehicle is introduced and this virtual vehicle is used as the tracking objective for the follower vehicle during cornering. The components of the look-ahead point s_{i-1} in Cartesian coordinates can be seen in equations (3.7) and (3.8). As mentioned before the magnitude of this extension vector needs to be determined such that vehicle i is cornering with the same turning radius as vehicle $i-1$, while it still maintains the effective inter-vehicle distance at $r_i + h_i v_i$. The magnitude $\bar{s}_{i-1}$ is determined by analyzing the steady-state behaviour of the platoon during cornering, where

it is assumed that the errors $e_{x,i}$ and $e_{y,i}$ are zero. In Figure 3.5 it can be seen that vehicle $i-1$ is turning towards the positive y-axis with a turning radius of R_{i-1}. The tracking objective for vehicle i is extended to point S.

The other problem that needs to be solved is that the vehicles in the platoon maintain the effective inter-vehicle distance. To guarantee a constant effective inter-vehicle distance between the vehicles the look-ahead distance l_a has to be redefined. When the vehicles are driving on a straight line the look-ahead distance is, according to the constant time-gap policy, equal to $r_i + h_i v_i$. Since the vehicles are driving on a straight line this look-ahead distance is equal to actual length of the path between the vehicles, so the effective inter-vehicle distance is maintained. To keep a constant effective inter-vehicle distance while cornering, the length of the path between the vehicles should be equal to $r_i + h_i v_i$ as can be seen in Figure 3.5. Note that the figure is similar to Figure 3.3, however modifications are made to the distance along the path and the projection of point S. This means that the look-ahead distance to point S needs to be redefined.

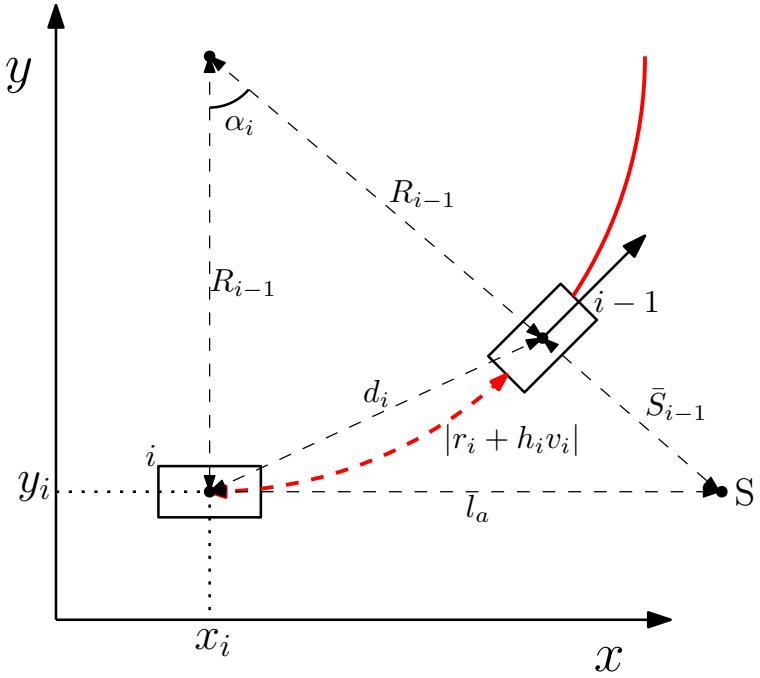

Figure 3.5: The magnitude of extension vector $\bar{s}_{i-1}$.

With this approach we force the length of the path between the vehicles to be always equal to $r_i + h_i v_i$, so we can guarantee that the effective inter-vehicle distance is maintained while driving on a straight line and while cornering. From Figure 3.5 it is obvious that the look-ahead vector changes during cornering when the length of the path between the vehicles has to be equal to $r_i + h_i v_i$. This leads to the following look-ahead distance:

$$l_a = \begin{cases} r_i + h_i v_i & \text{for } \kappa_{i-1} = 0 \\ \tan \alpha_i R_{i-1} & \text{for } \kappa_{i-1} \neq 0 \end{cases} \tag{3.24}$$

The angle of arc between vehicle i and $i-1$ is defined as α_i and can be determined with the turning radius R_{i-1} and the length of the path between vehicle i and $i-1$. Due to the spacing policy this length is equal to $r_i + h_i v_i$, this leads to the following equation:

$$\alpha_i = \frac{r_i + h_i v_i}{R_{i-1}} = (r_i + h_i v_i)\kappa_{i-1}, \quad -\frac{\pi}{2} < \alpha_i < \frac{\pi}{2} \tag{3.25}$$

With the angle of arc α_i, an expression for the magnitude of the extension vector $\bar{s}_{i-1}$ can be defined:

$$\bar{s}_{i-1} = \frac{R_{i-1}}{\cos \alpha_i} - R_{i-1} \tag{3.26}$$

When the vehicle is driving on a straight line, $\alpha_i = 0$, and thus the extension vector $\bar{s}_{i-1}$ is equal to zero. When the vehicle is cornering $\bar{s}_{i-1} \neq 0$ and thus the extension vector is applied to avoid corner-cutting behaviour.
With these expressions for the look-ahead distance and the magnitude of the extension vector the spacing error can be defined. The spacing error e_i for this extended look-ahead design is:

$$e_i = (p_{i-1} + s_{i-1}) - (p_i + l_a) \tag{3.27}$$

This position error can be decomposed in global Cartesian coordinates, the position error in x- and y-direction are used as the first and second state-component respectively. The third and the fourth state-component are the velocity error in x- and y-direction respectively. Following the approach of [1], the state-components are defined as:

$$z_{1,i} = x_{i-1} + s_{x,i-1} - x_i - l_a \cos \theta_i \tag{3.28}$$

$$z_{2,i} = y_{i-1} + s_{y,i-1} - y_i - l_a \sin \theta_i \tag{3.29}$$

$$z_{3,i} = v_{i-1} \cos \theta_{i-1} - v_i \cos (\theta_i + \alpha_i) \tag{3.30}$$

$$z_{4,i} = v_{i-1} \sin \theta_{i-1} - v_i \sin (\theta_i + \alpha_i) \tag{3.31}$$

Now the state-components of the controller are defined the controller inputs can be determined such that the desired behaviour is obtained. First the derivatives of α_i and $\bar{s}_{i-1}$ are derived:

$$\dot{\alpha}_i = p_{\kappa,i} \dot{\kappa}_{i-1} + p_{a,i} a_i \tag{3.32}$$

$$\dot{\bar{s}}_{i-1} = s_{\kappa,i} \dot{\kappa}_{i-1} + s_{\alpha,i} \dot{\alpha}_i \tag{3.33}$$

where

$$p_{\kappa,i} = r_i + h_i v_i \tag{3.34}$$

$$p_{a,i} = h_i \kappa_{i-1} \tag{3.35}$$

$$s_{\kappa,i} = -\frac{\sec \alpha_i - 1}{\kappa_{i-1}^2} \tag{3.36}$$

$$s_{\alpha,i} = \frac{\tan \alpha_i}{\cos \alpha_i \kappa_{i-1}} \tag{3.37}$$

The inter-vehicle dynamics can be obtained by differentiating the state-components with respect to time, which results in:

$$\begin{bmatrix} \dot{z}_1 \\ \dot{z}_2 \end{bmatrix} = v_{i-1} \begin{bmatrix} \cos \theta_{i-1} \\ \sin \theta_{i-1} \end{bmatrix} - v_i \begin{bmatrix} \cos \theta_i \\ \sin \theta_i \end{bmatrix} + \beta_{1,i} \begin{bmatrix} \sin \theta_{i-1} \\ \cos \theta_{i-1} \end{bmatrix} - \Gamma_{12,i} \begin{bmatrix} a_i \\ \omega_i \end{bmatrix} - \Lambda_{12,i} \tag{3.38}$$

$$\begin{bmatrix} \dot{z}_{3,i} \\ \dot{z}_{4,i} \end{bmatrix} = H_{i-1} \begin{bmatrix} a_{i-1} \\ \omega_{i-1} \end{bmatrix} - \Gamma_{34,i} \begin{bmatrix} a_i \\ \omega_i \end{bmatrix} + \beta_{2,i} \tag{3.39}$$

with

$$\beta_{1,i} = \begin{bmatrix} s_{\alpha,i} p_{\kappa,i} \dot{\kappa}_{i-1} + s_{\kappa,i} \dot{\kappa}_{i-1} & \bar{s}_{i-1} \omega_{i-1} \\ \bar{s}_{i-1} \omega_{i-1} & -s_{\alpha,i} p_{\kappa,i} \dot{\kappa}_{i-1} - s_{\kappa,i} \dot{\kappa}_{i-1} \end{bmatrix} \tag{3.40}$$

$$\beta_{2,i} = v_i \left(r_i + h_i v_i\right) \begin{bmatrix} \sin\left(\theta_i + \alpha_i\right) \\ -\cos\left(\theta_i + \alpha_i\right) \end{bmatrix} \dot{\kappa}_{i-1} \tag{3.41}$$

$$\Gamma_{12,i} = \begin{bmatrix} \cos\theta_i h_i & -(r_i + h_i v_i)\sin\theta_i \\ \sin\theta_i h_i & (r_i + h_i v_i)\cos\theta_i \end{bmatrix} \text{ for } \kappa_{i-1} = 0 \tag{3.42}$$

$$\Gamma_{12,i} = \begin{bmatrix} -s_{\alpha,i}\sin\theta_{i-1} p_{a,i} + \sec^2\alpha_i \cos\theta_i R_{i-1} p_{a,i} & -\tan\alpha_i R_{i-1}\sin\theta_i \\ s_{\alpha,i}\cos\theta_{i-1} p_{a,i} + \sec^2\alpha_i \sin\theta_i R_{i-1} p_{a,i} & \tan\alpha_i R_{i-1}\cos\theta_i \end{bmatrix} \text{ for } \kappa_{i-1} \neq 0 \tag{3.43}$$

$$\Gamma_{34.i} = \begin{bmatrix} \cos\left(\theta_i + \alpha_i\right) - \eta_i \sin\left(\theta_i + \alpha_i\right) & -v_i \sin\left(\theta_i + \alpha_i\right) \\ \sin\left(\theta_i + \alpha_i\right) + \eta_i \cos\left(\theta_i + \alpha_i\right) & v_i \cos\left(\theta_i + \alpha_i\right) \end{bmatrix} \tag{3.44}$$

$$\Lambda_{12,i} = \begin{bmatrix} \tan\alpha_i \cos\theta_i \dot{R}_{i-1} + \cos\theta_i \sec^2\alpha_i R_{i-1} p_{\kappa,i} \dot{\kappa}_{i-1} \\ \tan\alpha_i \sin\theta_i \dot{R}_{i-1} + \sin\theta_i \sec^2\alpha_i R_{i-1} p_{\kappa,i} \dot{\kappa}_{i-1} \end{bmatrix} \tag{3.45}$$

$$\eta_i = v_i h_i \kappa_{i-1} \cos^2\alpha_i \tag{3.46}$$

$$H_{i-1} := \begin{bmatrix} \cos\theta_{i-1} & -v_{i-1}\sin\theta_{i-1} \\ \sin\theta_{i-1} & v_{i-1}\cos\theta_{i-1} \end{bmatrix} \tag{3.47}$$

The objective of the controller is to asymptotically stabilize the state-components $[z_{1,i}, z_{2,i}, z_{3,i}, z_{4,i}]^T$ at zero. This is established when we take the feedback as:

$$\begin{bmatrix} a_i \\ \omega_i \end{bmatrix} = \Gamma_{12,i}^{-1}\Big(\begin{bmatrix} k_1 z_{1,i} \\ k_2 z_{2,i} \end{bmatrix} + v_{i-1}\begin{bmatrix} \cos\theta_{i-1} \\ \sin\theta_{i-1} \end{bmatrix} - v_i \begin{bmatrix} \cos\theta_i \\ \sin\theta_i \end{bmatrix} + \beta_{1,i}\begin{bmatrix} \sin\theta_{i-1} \\ \cos\theta_{i-1} \end{bmatrix} - \Lambda_{12,i}\Big) \tag{3.48}$$

This leads to the following closed-loop system:

$$\begin{bmatrix} \dot{z}_{1,i} \\ \dot{z}_{2,i} \end{bmatrix} = -\begin{bmatrix} k_1 z_{1,i} \\ k_2 z_{2,i} \end{bmatrix} \tag{3.49}$$

$$\begin{aligned} \begin{bmatrix} \dot{z}_{3,i} \\ \dot{z}_{4,i} \end{bmatrix} &= H_{i-1}\begin{bmatrix} a_{i-1} \\ \omega_{i-1} \end{bmatrix} + \beta_{2,i} - \Gamma_{34,i}\Gamma_{12,i}^{-1}\begin{bmatrix} k_1 z_{1,i} \\ k_2 z_{2,i} \end{bmatrix} \\ -\Gamma_{34,i}\Gamma_{12,i}^{-1}\Big(v_{i-1}&\begin{bmatrix} \cos\theta_{i-1} \\ \sin\theta_{i-1} \end{bmatrix} - v_i \begin{bmatrix} \cos\theta_i \\ \sin\theta_i \end{bmatrix} + \beta_{1,i}\begin{bmatrix} \sin\theta_{i-1} \\ \cos\theta_{i-1} \end{bmatrix} - \Lambda_{12,i}\Big) \end{aligned} \tag{3.50}$$

3.3.1 Stability analysis

It can be seen that by using the controller as in (3.48) a linear system (3.49) is obtained. By selecting $k_1, k_2 > 0$ the linear system (3.49) is exponentially stable, since in this case the system has eigenvalues which are strictly negative.

When the platoon is driving on a straight trajectory the subsystem (3.50) can be rewritten such that it is exactly the same as in [1]. Therefore it can be concluded from [1] that $\lim_{t\to\infty} ||z_{34,i}(t)|| = 0$ and thus the straight line case is stable. The proof can be found in Appendix A.

For the case where the platoon is driving with a constant velocity on a circular trajectory with a constant curvature it can be concluded that if κ_{i-1} is bounded with (3.51), we have that $\lim_{t\to\infty} ||z_{34,i}(t)|| = 0$.

$$|\kappa_{i-1}| < \frac{\cos^2\alpha_i}{h_i|\sqrt{2}\left(v_{i-1}^{\max} + v_{i-1}^{\min} - \varepsilon\right)\left(1 + \frac{1}{\sin\alpha_i} - \cos^3\alpha_i\right) - 2v_{i-1}^{\min}|} \tag{3.51}$$

The proof can be found in Appendix A.
Thus, it can be concluded that stability of the overall system for the case where the platoon is driving on a straight trajectory and for the case where the platoon is driving with a constant velocity on a circular trajectory with a constant curvature is established.

3.4 Controller comparison

In this section simulations with the extended look-ahead controller from [1] and the developed extended look-ahead controller from the previous section, that maintains the effective inter-vehicle distance at $r_i + h_i v_i$, are performed. First, a tracking performance measure is defined to be able to analyse and compare both controllers. Then the scenarios that are used for the simulations are described and after that simulations are performed. The extended look-ahead controller from [1] and the developed controller are simulated and the tracking performance of both controllers is compared.

3.4.1 Tracking performance measure

To verify the developed control approach and to be able to compare this approach with already existing control approaches a measure for tracking performance has to be defined. This tracking performance measure should analyse how well the follower vehicle tracks the leader vehicle of the platoon and it is important that this tracking performance is measurable. Since this tracking performance measure gives an indication of the quality of the developed controller it is important that this measure is well considered and accurate.

During this research a controller that maintains the actual length of the path between the vehicles equal to $r_i + h_i v_i$, according to the constant time-gap spacing policy, is developed. The main objective of the controller is to maintain the effective inter-vehicle distance at $r_i + h_i v_i$.

The discussed controllers in this research are developed in a global coordinate system, however it is much more intuitive to analyse the results in a local coordinate system. This means that the error in the local x-direction corresponds to the longitudinal error of the follower vehicle and that the local error in y-direction corresponds to the lateral error of the follower vehicle. To objectively evaluate the tracking performance of the follower vehicle, a local coordinate frame attached to this vehicle is used. The local x-axis points in the longitudinal direction of the follower vehicle and the local y-axis points in the lateral direction of the follower vehicle. In Figure 3.6 the local frame attached to vehicle i can be seen. With the moving frame we can express the relative position of vehicle $i-1$ with respect to vehicle i. This relative position does give some useful information, however without information about the trajectory no conclusions can be drawn. To express how well the follower vehicle tracks the preceding vehicle another method is proposed. Ideally, the positions of both vehicles are exactly the same when we compare the position of vehicle i with the position of vehicle $i-1$ when this vehicle has driven $(r_i + h_i v_i)$ meters less than vehicle i. This is because the controller should maintain an effective inter-vehicle distance of $(r_i + h_i v_i)$ at all times. Since the positions of both vehicles are known at all times, we can compare the position of vehicle i with the position of vehicle $i-1$ that corresponds to the driven distance of this vehicle minus $(r_i + h_i v_i)$. In other words, the position of vehicle $i-1$ is transformed backwards with the desired distance $r_i + h_i v_i$ and compared with the position of vehicle i as can be seen in Figure 3.6.

With the backtransformed vehicle $i-1$ the difference in both position and heading between vehicle i and the backtransformed vehicle $i-1$ can be calculated, this leads to the longitudinal error e_x, the lateral error e_y and the heading error e_θ as indicated in the figure.

The performance of the controllers is expressed in three values now, but to compare different controllers it is convenient to express the performance of the controllers in one value, this leads to the following equation:

$$e(t) = \sqrt{e_x^2(t) + e_y^2(t)} \tag{3.52}$$

This expression is used to analyse the tracking performance of the different controllers in this report. The tracking performance measure takes the effective inter-vehicle distance into account and consists of the local x- and y-error, so at every time-step it can be seen how much the

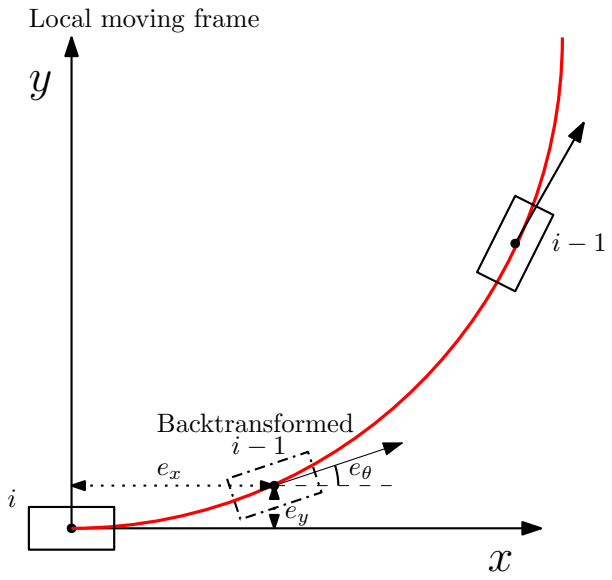

Figure 3.6: The tracking performance measure with a local coordinate system and the backtransformed vehicle $i-1$.

longitudinal and lateral error contributes to the total tracking performance measure and from that conclusions can be drawn. The heading angle error is neglected in the equation, since it is more intuitive to have a performance measure that consists of only position errors instead of a combination of position errors and a heading angle error.

3.4.2 Scenarios

In the previous sections the extended look-ahead controllers are elaborated and a tracking performance measure is defined. To simulate the extended look-ahead controllers two different scenarios are used:

- Driving on a straight trajectory with a velocity of 5 m/s, after t = 5 s accelerate with an acceleration of 2.40 m/s^2 to 7.5 m/s and after t = 18 s decelerate with a deceleration of 2.40 m/s^2 to 5 m/s again.
- Driving on a straight trajectory with a constant velocity of 5 m/s and after t = 6 s the platoon enters a double lane roundabout with a radius of 12.5 m.

The first scenario is the simplest scenario, in this scenario the platoon does not corner, so there is only longitudinal vehicle following. The platoon consists of three vehicles and the vehicles in the platoon start without an initial spacing error and the initial heading angle is 0 rad. The initial velocity of the vehicles is 5 m/s, at t = 5 s vehicle 1 starts accelerating until it reaches a velocity of 7.5 m/s and at t = 18 s vehicle 1 decelerates to 5 m/s again, the velocity profile of vehicle 1 can be seen in Figure 3.7.
With this scenario it can be verified that the developed extended look-ahead controller works as expected, since no differences with the extended look-ahead controller from [1] should be observed. Furthermore, the performance measure that is defined in the previous section can be verified. In this scenario the vehicles are not cornering and thus it is expected that the lateral error is always zero. The longitudinal error should be zero initially and when the vehicles start accelerating small errors may be observed. Eventually these small errors should converge to zero for all vehicles in the platoon.

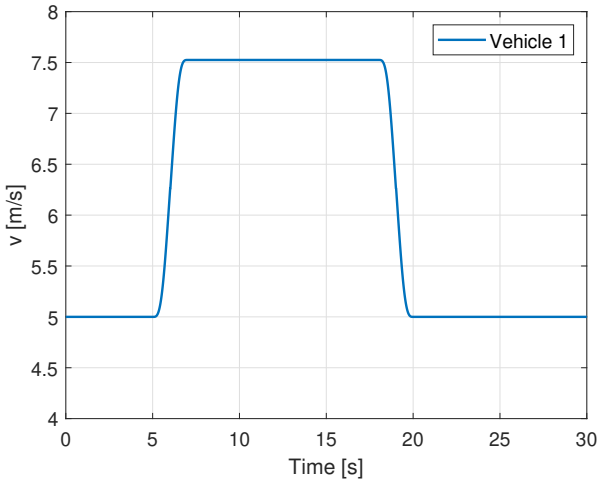

Figure 3.7: The velocity profile for vehicle 1 in the platoon.

In the second scenario longitudinal and lateral vehicle following are evaluated for both controllers. In this scenario the platoon, consisting of three vehicles, is driving on a straight trajectory with a velocity of 5 m/s and after t = 6 s the platoon enters the inner lane of a double lane roundabout. The dimensions of a double lane roundabout in the Netherlands according to [31] can be found in Table 3.1. The vehicles in the platoon enter the inner lane of a roundabout with the smallest possible dimensions, which means that the vehicles corner with a turning radius of 12.5 m. The trajectory that is prescribed to vehicle 1 can be seen in Figure 3.8.
In this scenario differences between both controllers should be observed, since the extended look-ahead controller from [1] cruises with a smaller effective inter-vehicle distance and thus there is a longitudinal error for this controller. The developed extended look-ahead controller should maintain the effective inter-vehicle distance at $r_i + h_i v_i$, so the longitudinal error should converge to zero.

Table 3.1: Dimensions for two lane roundabouts in the Netherlands [31]

Design element	Minimum	Maximum
Outer radius	20 m	38 m
Inner radius	10 m	30 m

3.4.3 Simulation results

Straight trajectory

In the first scenario the platoon is driving on a straight trajectory and the platoon consist of three vehicles. The spacing policy parameters are $r_i = 0.5$ m and $h_i = 1$ s, the control parameters $k_1 = k_2 = 3.5$ are chosen. Various gains are tested and the results show that with low controller gains it takes longer for the follower vehicles to converge to the path of their preceding vehicle and thus it takes longer for the tracking errors to stabilize, especially when the vehicles start with an initial spacing error. On the other hand, with high controller gains the follower vehicles are converging faster to the path of their preceding vehicle and therefore the tracking errors are stabilizing faster. However, with high controller gains the controller is more sensitive for disturbances, such as accelerations and varying yaw-rates. In practical situations measurement noise or inaccurate measurements could lead to overreacting of the controller with high controller gains. In simulations it is assumed that there is no measurement noise or inaccurate measurements, furthermore

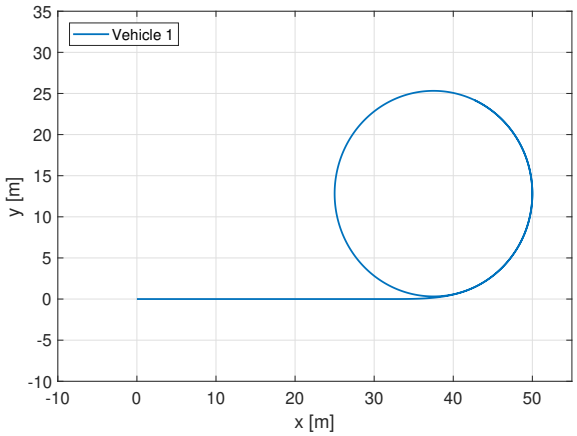

Figure 3.8: The trajectory of vehicle 1 for the double lane roundabout scenario.

the vehicles are positioned without an initial spacing error. Therefore, higher controller gains are possible, but to compare both controllers the gains from [1] are adopted. With these controller gains a fast convergence of the follower vehicles towards the path of their preceding vehicle is seen and by selecting these controller gains we avoid the discussion that one of the controller performs better due tuning of the controller gains. The initial positions for the vehicles are (0 m, 0 m), (-5.5 m, 0 m) and (-11 m, 0 m) for vehicles 1,2 and 3 respectively, this means that the vehicles start without an initial spacing error according to the constant time-gap spacing policy. The vehicles start with an initial heading angle $\theta_i = 0$ rad for all vehicles. The acceleration and yaw-rate profiles corresponding to this scenario are used as a direct input for vehicle 1, while the extended look-ahead controller from [1] and the developed extended look-ahead controller are implemented in the other vehicles. In the simulations it is assumed that the vehicles can communicate the position, heading, velocity and acceleration without delays.

In Figure 3.9 the velocity of the vehicles in the platoon can be seen for both controllers. As expected both controllers show the exact same behaviour, this is because the controllers are modelled the same way when the platoon is driving on a straight trajectory. It can be seen that the velocity of vehicle 2 and 3 converges to 7.5 m/s after the acceleration of vehicle 1 for both controllers, the same convergence to 5 m/s for vehicle 2 and 3 can be seen when vehicle 1 decelerates to 5 m/s again.

The RMS tracking error according to (3.52) is calculated for both controllers with the following equation:

$$\text{RMS} = \sqrt{\frac{1}{K}\sum_{k=1}^{K} e(t)^2} \tag{3.53}$$

Here K is the number of samples. In Table 3.2 the RMS tracking errors are depicted for both controllers, from this table it becomes clear that the RMS tracking errors are almost equal to zero, which means that both controllers perform well and as expected when the vehicles are driving on a straight trajectory.

Double lane roundabout

In this case the platoon is driving on a straight trajectory with an initial velocity of 5 m/s. Vehicle 1 enters the inner lane of a double roundabout at time t = 6 s, which means that the turning radius

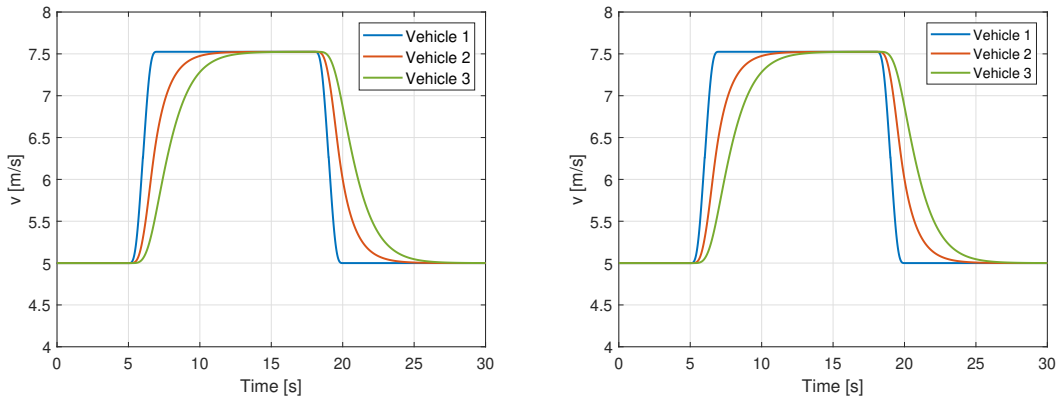

Figure 3.9: The velocity of the vehicles in the platoon for the straight trajectory: extended look-ahead controller from [1] (left) and the developed extended look-ahead controller (right).

Table 3.2: The RMS tracking errors for the controller from [1] and the developed controller.

	RMS tracking error for the controller from [1]	RMS tracking error for the developed controller
Vehicle 1	0 [m]	0 [m]
Vehicle 2	$9.65 \cdot 10^{-4}$ [m]	$9.65 \cdot 10^{-4}$ [m]
Vehicle 3	$9.19 \cdot 10^{-4}$ [m]	$9.19 \cdot 10^{-4}$ [m]

of this vehicle becomes 12.5 m according to [31]. The spacing policy parameters are $r_i = 0.5$ m and $h_i = 1$ s and the control parameters $k_1 = k_2 = 3.5$ are chosen using the same reasoning as for the straight trajectory. The initial positions for the vehicles are (0 m, 0 m), (-5.5 m, 0 m) and (-11 m, 0 m) for vehicles 1,2 and 3 respectively, this means that the vehicles start without an initial spacing error according to the constant time-gap spacing policy. The vehicles start with an initial heading angle $\theta_i = 0$ rad for all vehicles. The acceleration and yaw-rate profiles corresponding to this scenario are used as a direct input for vehicle 1, while the extended look-ahead controller from [1] and the developed extended look-ahead controller are applied in the other vehicles to follow their preceding vehicle. In the simulations it is assumed that the vehicles can communicate the position, heading, velocity and acceleration without delays.

In Figure 3.10 the trajectory of the vehicles in the platoon can be seen for both controllers. From the figure it can be seen that both controllers perform well on the straight trajectory and as expected there is no lateral error. However, it can be seen that vehicle 2 and 3 steer slightly away from their preceding vehicle just before they enter the roundabout. This behaviour is seen for both controllers and it can be explained by how the extended look-ahead point S is defined. At the moment vehicle 1 starts cornering, $\omega_1 \neq 0$ rad/s, and thus the look-ahead point extends from vehicle 1. Because vehicle 1 just started cornering and did not made significant lateral movement yet, the extended look-ahead point S is located below the positive global x-axis. Vehicle 2 tracks this extended look-ahead point S and steers towards the negative global y-axis as can be seen in the figure. In Figure 3.11 the trajectory of vehicle 1 and point S extending from vehicle 1 that acts as a reference for vehicle 2 are plotted for the developed controller. From the figure it can be seen that point S extends below the positive x-axis and this causes the steering behaviour of vehicle 2. The same phenomenon can be seen for vehicle 3 in the platoon. Eventually all vehicles in the platoon drive with the same turning radius as their preceding vehicle and no corner-cutting behaviour is observed.

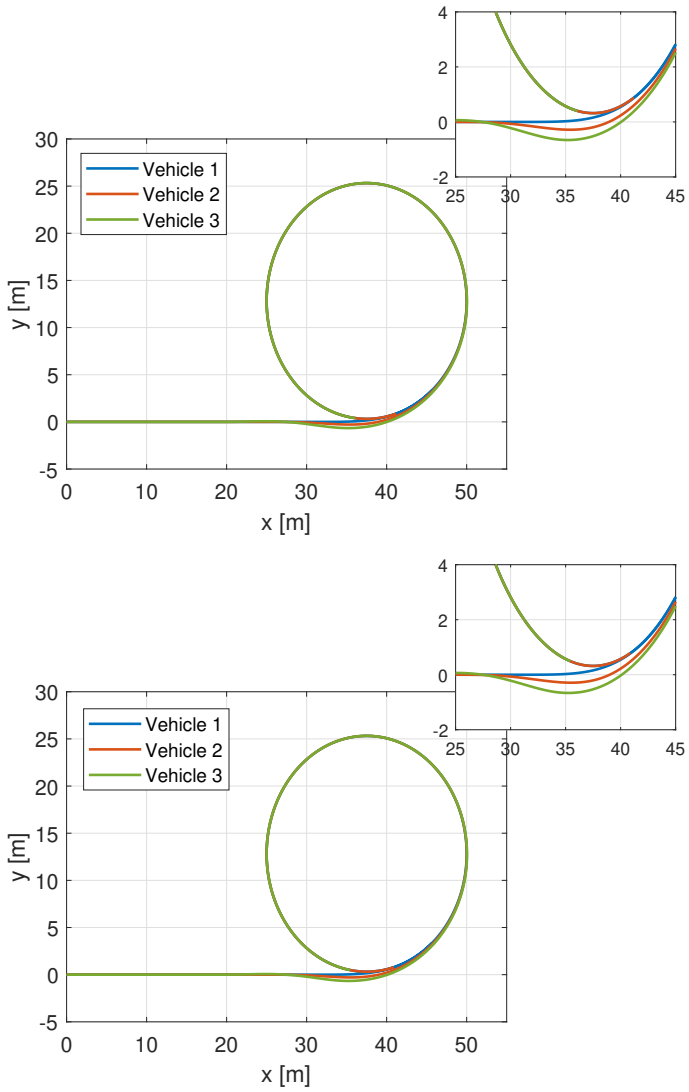

Figure 3.10: The trajectory of the vehicles in the platoon for the double lane roundabout: extended look-ahead controller from [1] (top) and the developed extended look-ahead controller (bottom).

In Figure 3.12 the tracking error according to (3.52) is depicted for both controllers. From this figure it can be observed that both controllers have a peak in the error starting from t = 6 s. The difference between the controllers is that the extended look-ahead controller from [1] converges to a tracking error of 0.32 m, while the tracking error of the developed controller converges to zero. In Table 3.3 the RMS tracking errors are depicted for both controllers. From this table it can be seen that the RMS tracking error is significantly larger for the extended look-ahead controller from [1].

In Figure 3.13 the longitudinal and lateral tracking errors are depicted separately for both controllers. From this figure it becomes clear that the lateral error starting from $t = 6$ s is roughly the same for both controllers, but clear differences in the longitudinal error can be seen.
For the extended look-ahead controller from [1] a lateral error starting from $t = 6$ s can be seen, this lateral error is caused by the fact that the tracking objective for the follower vehicles extends to point S, even while their preceding vehicle did not make any significant lateral movement. This makes the follower vehicle steer "away" before it enters the roundabout, this leads to a lateral

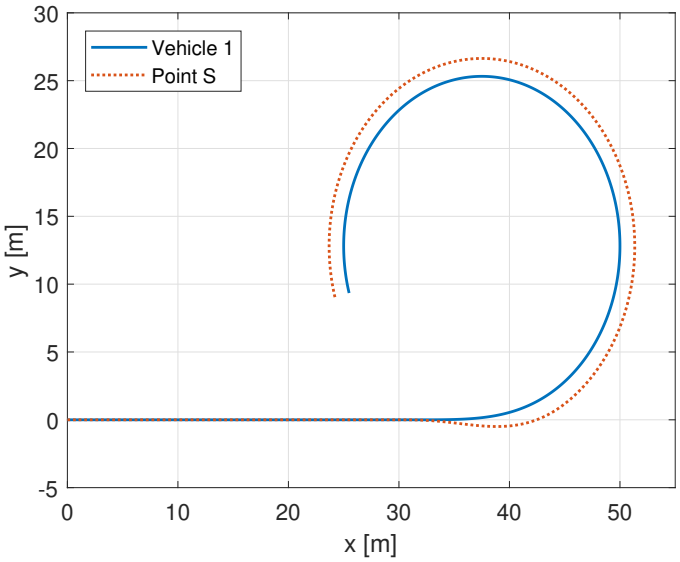

Figure 3.11: The trajectory of vehicle 1 and the point S extending from vehicle 1 for the double lane roundabout scenario for the developed controller.

error as can be seen in the figure. What stands out is that the longitudinal error converges to -0.32 m during cornering. From this figure it can be concluded that the performance error from Figure 3.13 is caused by both the longitudinal and lateral error initially. Eventually the lateral error converges to zero and from that moment the tracking error is caused by the longitudinal error only. So, the extended look-ahead controller from [1] successfully compensates for corner-cutting, but this controller does not maintain the effective inter-vehicle distance at $r_i + h_i v_i$ during cornering. For the developed extended look-ahead controller roughly the same lateral error can be seen from $t = 6$ s, which is again caused by the extended look-ahead point S. A small peak in the longitudinal error can be seen after which the longitudinal error converges to zero. The small peak in the longitudinal error is also caused by steering away of the follower vehicles as explained before. From this figure it can be seen that the tracking error from Figure 3.12 is mainly caused by the lateral error, while there is no significant contribution of the longitudinal error. The longitudinal error converges to zero, so it can be concluded that the developed controller successfully compensates for corner-cutting behaviour, while it maintains the effective inter-vehicle distance at $r_i + h_i v_i$ during cornering.
It should be noted that the tracking error of the extended look-ahead controller from [1] is not because of a tuning of the controller gains, but is caused by the reference that is applied to the controller. The controller gains affect how fast the controller converges to its reference and how sensitive the controller is for curvature changes. However, the extended look-ahead controller from [1] always converges to a certain tracking error during cornering, while the tracking error of the developed controller always converges to zero during cornering.

Table 3.3: The RMS tracking errors for the controller from [1] and the developed controller.

	RMS tracking error for the controller from [1]	RMS tracking error for the developed controller
Vehicle 1	0 [m]	0 [m]
Vehicle 2	0.30 [m]	0.09 [m]
Vehicle 3	0.29 [m]	0.09 [m]

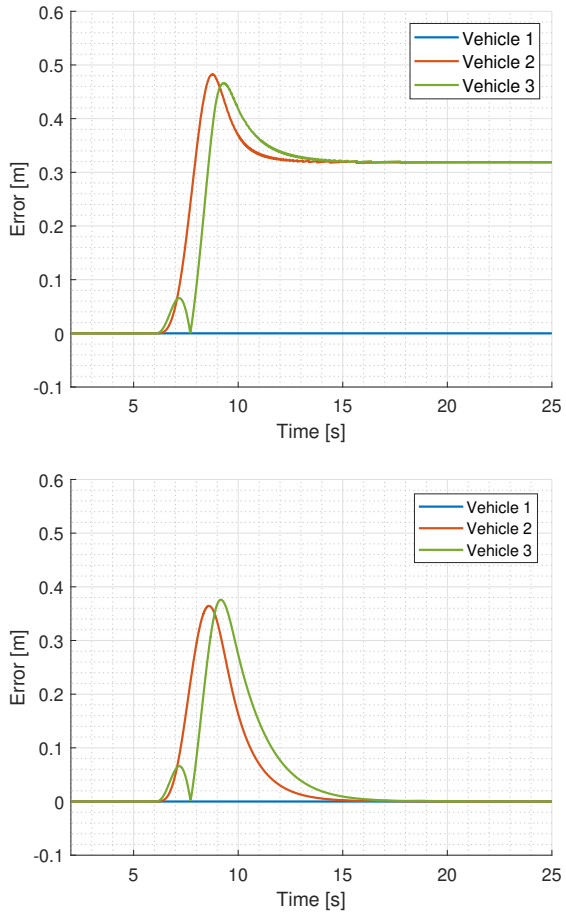

Figure 3.12: The tracking error according to (3.52) of the vehicles in the platoon for the double lane roundabout: extended look-ahead controller from [1] (top) and the developed extended look-ahead controller (bottom).

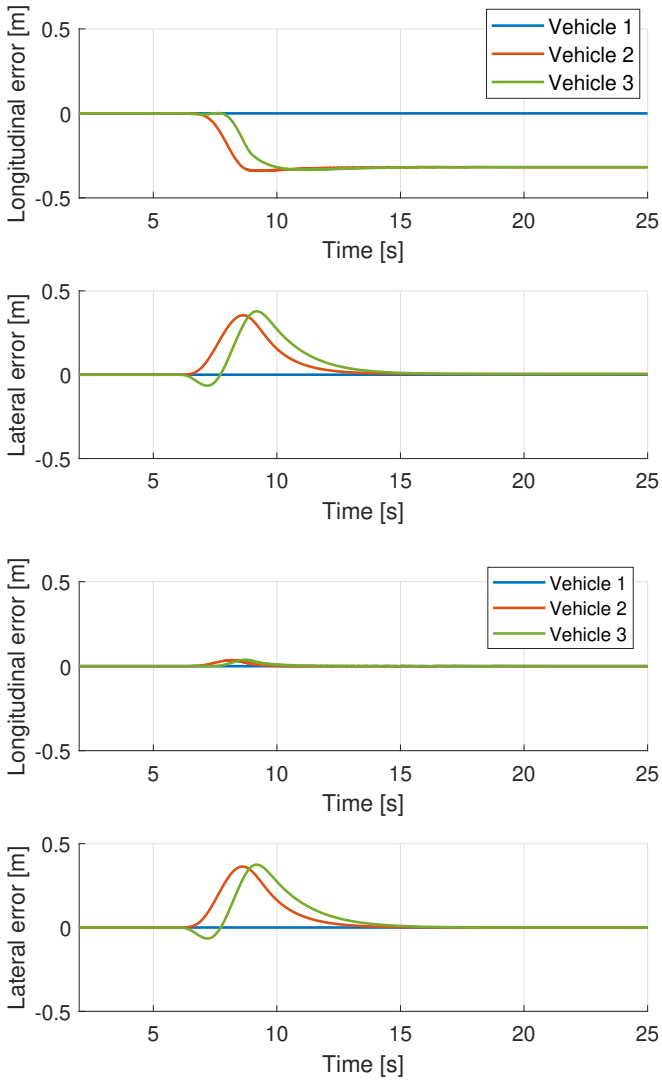

Figure 3.13: The longitudinal and lateral tracking error of the vehicles in the platoon for the double lane roundabout: extended look-ahead controller from [1] (top) and the developed extended look-ahead controller (bottom).

3.5 Conclusions

In this chapter the extended look-ahead controller that is developed in [1] is discussed. Here a method to compensate for corner-cutting behaviour of conventional look-ahead controller is introduced. A virtual vehicle that extends from the base of the preceding vehicle during cornering maneuvers acts as the tracking objective for the follower vehicle and the effectiveness of this extended look-ahead point is shown in simulations. The problem with this extended look-ahead controller is that variations in inter-vehicle distance are seen, which leads to unintended accelerations in longitudinal direction. It is shown that the effective inter-vehicle distance decreases for a decreasing turning radius and an increasing time-gap. Therefore, a vehicle following controller with extended look-ahead is developed. It is shown that with this controller stability of the overall system is established for the cases where the platoon is driving on a straight trajectory and when the platoon is driving with a constant velocity on a circular trajectory with a constant curvature. This controller compensates for the corner-cutting behaviour, while it maintains the effective inter-vehicle distance at $r_i + h_i v_i$. A tracking performance measure is proposed, this measure analyses how well the follower vehicle tracks the preceding vehicle. Simulations show that the extended look-ahead controller from [1] and the developed controller have the same behaviour and performance for driving on a straight trajectory. When the platoon is cornering differences between the controllers are observed. The extended look-ahead controller from [1] cruises with a significant longitudinal spacing error during cornering, while the longitudinal spacing error of the developed controller converges to zero. However, both controllers show a lateral error when the platoon starts cornering. This is caused by the extended look-ahead point, which also extends when the vehicle did not made significant lateral movement yet. However, this lateral error converges to zero over time.

Chapter 4

Test vehicle and measurements

In this chapter the practical set-up with the Renault Twizys is discussed. First, the extended look-ahead controller from [1] and the developed controller are implemented in the Renault Twizys. Where vehicle-to-vehicle wireless communication is used to obtain the relevant states of the vehicle. The controller outputs are the acceleration and the yaw-rate of the follower vehicle, these outputs are converted to a gas pedal position and a steering angle. Then a control panel is developed to allow for real-time changes in the control parameters. After that experiments with the two Twizys are performed at a vehicle test centre facility and the results are analysed.

4.1 Practical set-up

This research is part of the integrated Cooperative Automated VEhicles (i-Cave) program [9], this program researches automated and cooperative driving. In this program a Cooperative Dual Mode Automated Transport (C-DMAT) system is researched and designed, which results in dual mode vehicles where the driver is able to choose between automated or manual driving. For this program the C-DMAT system is implemented in Renault Twizys. The Renault Twizy is a two-seater, compact, electric powered city vehicle. In the rear wheel driven Twizy the driver and the passenger sit in line instead of next to each other. This makes the Twizy very compact with a width of 1.4 m and a length of 2.3 m.
In the Automotive lab at the TU Eindhoven there are three Twizys present at this moment. One Renault Twizy is unmodified yet and therefore this vehicle cannot be used in this research. The other two Twizys are equipped with custom sensors and actuators, these sensors and actuators are connected to a MATLAB based real-time control system. These two modified Renault Twizys can be seen in Figure 4.1. The extended look-ahead controller from [1] and the developed controller are implemented in the two modified Renault Twizys. For safety reasons and lack of permission to drive on public roads, experiments with the Renault Twizys are carried out at “Leeuw Trainingscentrum” in Eindhoven.

Figure 4.1: The two modified Renault Twizys [32].

4.2 Implementation of the controller

In this section the most important steps taken to implement the controllers in the Renault Twizys are elaborated. First, communication of the relevant states between the vehicles is established. Then the controllers are implemented and after that kinematic steering is used to convert the yaw-rate in a steering-angle. Finally, a control panel is designed that is used during the experiments.

4.2.1 Vehicle-to-vehicle Communication

In the Automotive lab there are two Renault Twizys that are equipped with extra sensors and actuators, therefore these vehicles can be used for direct vehicle following. Twizy 2 is the upgraded version of Twizy 1, since more advanced equipment is installed on Twizy 2. Consequently, Twizy 1 is the leader vehicle that is driven manually and Twizy 2 is the follower vehicle in which the extended look-ahead controllers are implemented.
Vehicle-to-vehicle communication is a technique that allows vehicles to wirelessly receive and broadcast relevant information from and to other vehicles, such as speed, heading and position. The following relevant states of Twizy 1 are communicated through vehicle-to-vehicle wireless communication via Wi-Fi P (ITS-G5) to Twizy 2:

- Position (x, y) of Twizy 1
- Heading θ of Twizy 1
- Velocity v_x of Twizy 1
- Yaw-rate ω_z of Twizy 1

4.2.2 Controller implementation

With the implementation of the controller another problem arises, since the available sensors have limited update rates and are affected by measurement noise. In [33] a cooperative state estimation network is developed that provides detailed information of the relevant state-components, which can be used as controller inputs in a longitudinal and lateral platooning framework [33]. The state-estimator from [33] is used in order to estimate the states of Twizy 1 and Twizy 2 simultaneously. As part of the i-Cave program the state-estimator from [33] is developed and implemented

in the Simulink model of the Renault Twizy. For further information about the state-estimator the reader is referred to [33].

The extended look-ahead controller from [1] and the developed extended look-ahead controller are both implemented in the Simulink model of the Renault Twizy. The controller outputs are the vehicle's acceleration and yaw-rate. The acceleration output can be directly used as an input for the longitudinal acceleration controller that is developed as part of the i-Cave program.
The yaw-rate controller output first has to be converted into a steering angle before it can be used as an input for the steer controller that is developed as part of the i-Cave program. The conversion from yaw-rate into a steering angle is elaborated in the next subsection.

4.2.3 Steering angle

One of the controller outputs is the yaw-rate of Twizy 2 in order to follow Twizy 1 without a tracking error, this yaw-rate needs to be converted into a steering angle reference for the steer controller. For this conversion the linear single track vehicle model is used, in this model the left and the right tyre and axle characteristics are lumped into one single tyre. These equivalent tyres are linked by the body of the vehicle, a simplification of the single track vehicle model can be seen in Figure 4.2. For this model the following assumptions are made [22]:

- The left and right tyre and axle characteristics are lumped in one equivalent tyre
- Body roll is neglected
- Centre point steering
- Constant forward velocity
- Aerodynamic forces are neglected

The single track vehicle model allows the investigation of the fundamental driving dynamics if the lateral acceleration does not exceed 4 m/s^2 on dry roads [34]. Since the experiments are performed at low speeds with low lateral accelerations, the lateral acceleration does not exceed 4 m/s^2, thus this vehicle model can be used.

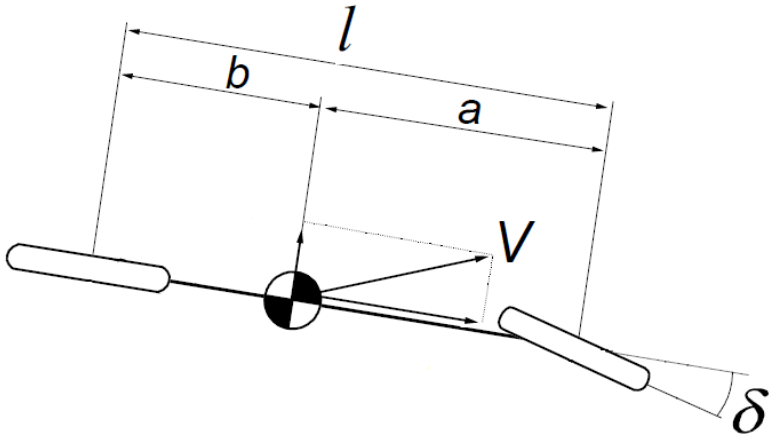

Figure 4.2: The single track vehicle model [34].

By considering the steady-state single track equations of motion an expression for the steering angle can be derived [22]:

$$\delta = \frac{l}{R} - \frac{mV^2}{Rl}\left(\frac{a}{C_2} - \frac{b}{C_1}\right) \tag{4.1}$$

In this equation l is the wheelbase of the vehicle, R is the turning radius, m is the mass of the vehicle, V is the velocity of the vehicle, a is the distance from the center of gravity to the front wheel, b is the distance from the center of gravity to the rear wheel, C_1 is the cornering stiffness of the front wheel and C_2 is the cornering stiffness of the rear wheel. The equation can be rewritten by substituting (3.10):

$$\delta = \frac{l\omega_z}{V} - \frac{m\omega_z V}{l}\left(\frac{a}{C_2} - \frac{b}{C_1}\right) \tag{4.2}$$

With this equation an expression for the steering angle as a function of the yaw-rate is found. The required vehicle parameters can be seen in Table 4.1.

Table 4.1: The vehicle parameters of the Renault Twizy.

Vehicle parameter	**Name**	**Value**
l	Wheelbase	1.68 m
m	Mass of the vehicle	708 kg
a	Distance from center of gravity to front wheel	0.93 m
b	Distance from center of gravity to rear wheel	0.75 m
C_1	Cornering stiffness front wheel	46333 N/rad
C_2	Cornering stiffness rear wheel	34252 N/rad

The equations are implemented in the Simulink model, so the controller output ω_z can be converted into a steering angle. This steering angle reference goes into the steer controller of the Renault Twizy.

4.2.4 Control panel

A control panel that is linked with Simulink Real-Time is developed. With Simulink Real-Time a real-time application is created from the Simulink model that is described in the previous subsections and runs it on the target computer that is connected to the Renault Twizy.
This control panel allows for real-time changes in the control parameters for example, without building the entire Simulink model again. The part of the control panel that is used for experiments with the extended look-ahead controllers can be seen in Figure 4.3.
The control panel allows us to change between the extended look-ahead controller from [1] and the developed extended-look-ahead controller. The controller gains k_1 and k_2 can be changed even as the standstill distance r_i and the time-gap h_i. Furthermore, the control panel gives us information about the controller outputs a and ω_z and if the extended look-ahead controller is turned on.
The displayed controller outputs are used to position the vehicles at the start of the experiments. When the vehicles are positioned without an initial spacing error, the controller outputs should be zero or close to zero.

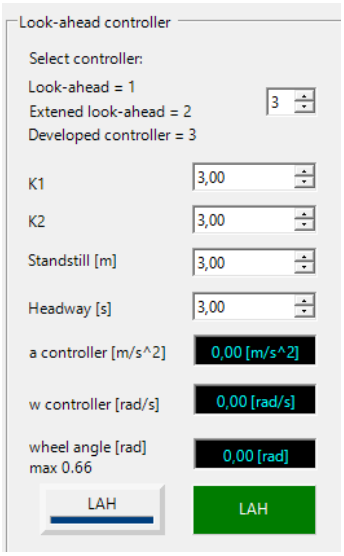

Figure 4.3: The control panel.

4.3 Experiments

In this section the results of the experiments with the Renault Twizys are discussed. For these experiments three reference trajectories are defined: a straight trajectory, a slalom and a trajectory with a turn to the right. Twizy 1, the leader vehicle, is driven manually, while the extended look-ahead controllers are applied on Twizy 2. Traffic cones are used in order to define the trajectory for Twizy 1, which ensures that Twizy 1 drives roughly the same trajectory each measurement. The controller outputs displayed in the control panel are used to position Twizy 2 without an initial spacing error behind Twizy 1. The control parameters $k_1 = k_2 = 1.5$ are chosen. To determine the controller gains for the experiments we start with controller gains close to zero and increase those gains with small steps of 0.1. Results show that with higher controller gains Twizy 2 converges faster to the path of Twizy 1, but this also leads to a controller that is more sensitive to measurement noise and this results in overcompensation. Thus for the selection of the controller gains we look into the magnitude of the tracking errors, but more important controller gains are selected by which we both feel safe and comfortable in the vehicle. It should be noted that we are both sitting in the Renault Twizy with a laptop to monitor and operate the controller, while we have to scan the environment for hazard.

4.3.1 Straight trajectory

In the first scenario Twizy 1 drives on a straight trajectory and starts from standstill. Twizy 1 accelerates with an acceleration of 0.6 m/s^2 until it reaches a velocity of 3 m/s and maintains this velocity for 5 seconds. Then the vehicle accelerates with an acceleration of 0.4 m/s^2 to 5 m/s. Twizy 1 maintains this velocity for 5 seconds again and then the vehicle is stopped. Twizy 2 is positioned without an initial spacing error behind Twizy 1 according to the constant time-gap spacing policy, this is done by using the displayed controller outputs on the control panel. The spacing policy parameters are selected as $r_i = 6$ m and $h_i = 0.5$ s for this scenario.

In Figure 4.4 the trajectories of Twizy 1 and Twizy 2 are shown for the extended look-ahead controller from [1] and the developed controller. Here the vehicles start from the left-hand side and are driving towards the right. From the figure it can be seen that both vehicles are not driving in a straight line, even though Twizy 1 is driven manually and the track is straight. It can be seen that for both controllers the trajectories of both vehicles deviate in the beginning and around x

= 35 m the trajectories of the vehicles start coming closer together.
The velocity of both vehicles can be seen in Figure 4.5 for both controllers. It can be seen that Twizy 1 starts from standstill and accelerates to a velocity of 3 m/s. This velocity is maintained for about 5 seconds and then the vehicle accelerates to 5 m/s. This velocity is maintained again for 5 seconds and after that the vehicle is stopped. The figure shows that Twizy 2 roughly follows this velocity profile, but clear deviations can be seen. For the extended look-ahead controller from [1] large oscillations can be seen between 2 and 8 seconds, after that the velocity stabilizes and Twizy 2 follows the velocity profile of Twizy 1. For the developed controller two peaks can be seen initially, however after 4 seconds the vehicle is able to follow the velocity of Twizy 1 with small deviations.

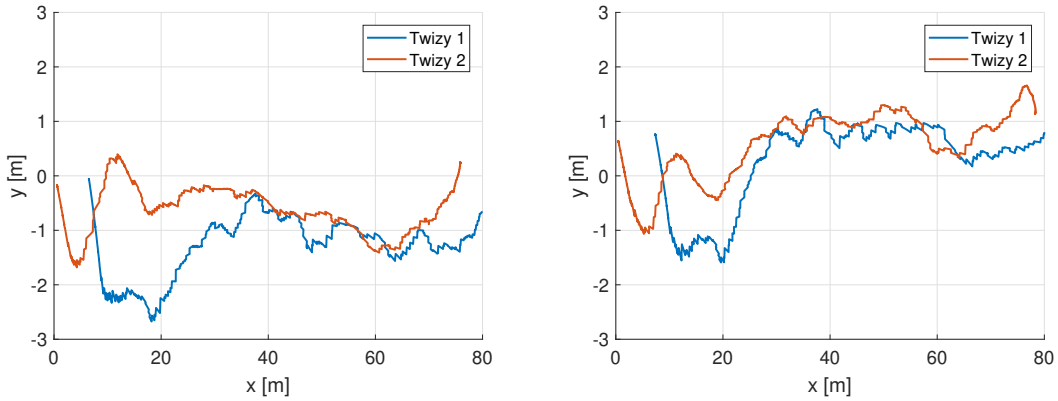

Figure 4.4: Trajectory of the Twizys: extended look-ahead controller from [1] (left) and the developed extended look-ahead controller (right).

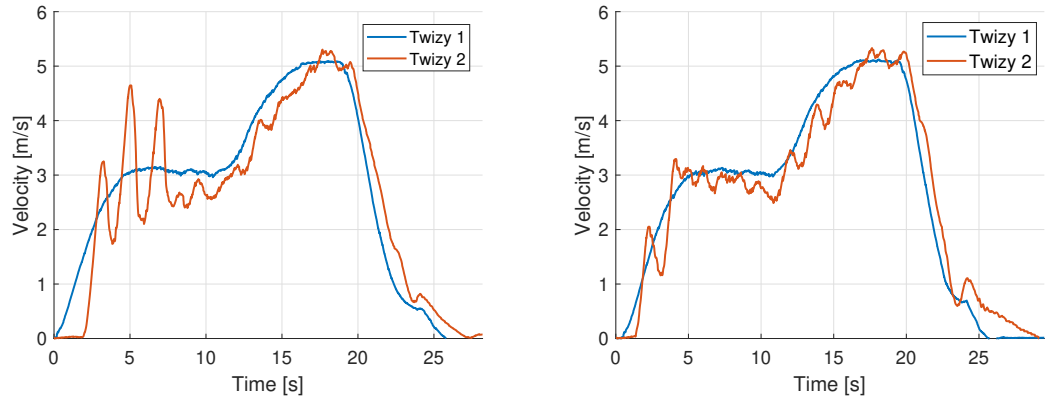

Figure 4.5: Velocity of the Twizys: extended look-ahead controller from [1] (left) and the developed extended look-ahead controller (right).

In Figure 4.6 the tracking error as defined in (3.52) is depicted for both controllers. The longitudinal and lateral tracking error of Twizy 2 for both controllers can be seen in Figure 4.7. It can be seen that both controllers start with an initial tracking error, despite the fact that the vehicles are positioned without an initial spacing error. Large variations in the tracking error are observed for both controllers. However, the tracking error does not exceed 2.9 m for the extended

look-ahead controller from [1] and for the developed controller this tracking error does not exceed 2.3 m. What stands out is that the tracking error is small between 14 and 20 seconds for both controllers, this corresponds to the interval where Twizy 1 is driving with a constant velocity of 5 m/s. In the figures high frequency errors can be seen, those errors are from the noisy position measurements as can be seen in Figure 4.4. Furthermore, for the performance measure Twizy 1 is backtransformed with the distance $r_i + h_i v_i$, since the sensors have a certain update rate the driven distance of vehicle $i-1$ subtracted by $r_i + h_i v_i$ may not exist. So the position that is closest to this driven distance is used and this may amplify the signal noise on the tracking errors. The RMS tracking error of the extended look-ahead controller from [1] is 1.28 m, while the RMS tracking error of the developed controller is 0.98 m. Thus, what stands out is that the RMS tracking error is smaller for the developed controller for the straight trajectory.

An explanation for the velocity oscillations at the beginning of the experiments for the extended look-ahead controller from [1] is that Twizy 2 only starts driving after about 2 seconds. Twizy 2 starts with a relatively small tracking error, however this tracking error increases during the first two seconds since Twizy 2 is still standing still. To compensate for this longitudinal tracking error Twizy 2 starts accelerating and an overshoot can be seen. The delay after which Twizy 2 starts driving can be explained by the fact that the controller needs to be turned on manually after which you have to enable the steering wheel and the driveline manually. This takes some time after which Twizy 2 can start driving autonomously. During this delay the tracking error increases and the controller compensates aggressively for this tracking error. For the initial peaks at the beginning of the measurement for the developed controller the same explanation holds. However the delay is shorter, but Twizy 2 starts with an initial longitudinal spacing error at the beginning of the experiment.

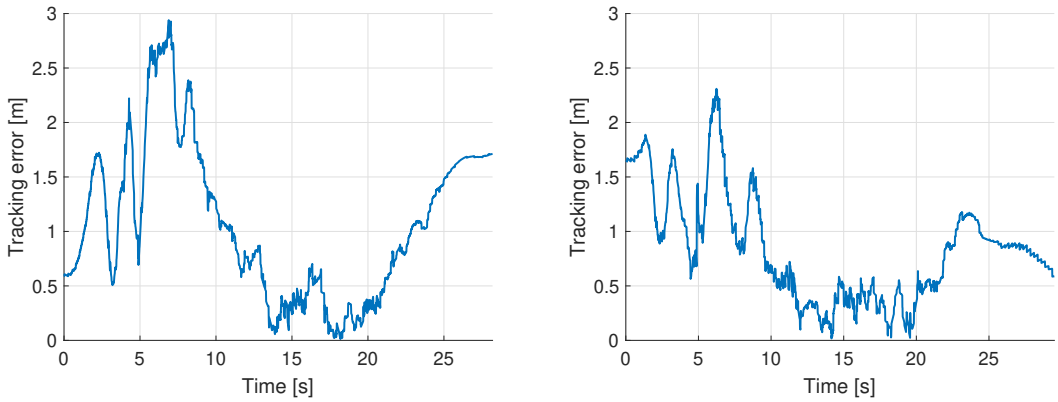

Figure 4.6: Tracking error of Twizy 2: extended look-ahead controller from [1] (left) and the developed extended look-ahead controller (right).

4.3.2 Slalom trajectory

In this scenario a slalom is performed with the Twizys, traffic cones are used so the driver of Twizy 1 knows where to corner. Twizy 1 starts from standstill and Twizy 2 is positioned without an initial spacing error behind this vehicle. Twizy 1 accelerates with 1 m/s^2 until it reaches a velocity of 5 m/s. At $t = 7$ seconds Twizy 1 starts with the slalom and stops when it reaches the end of the road. The spacing policy parameters are chosen as $r_i = 8$ m and $h_i = 0.5$ s for this scenario.

In Figure 4.8 the trajectory of both vehicles can be seen for the slalom. From this figure it can

be observed that for both controllers Twizy 2 roughly follows the slalom of Twizy 1. The slalom shape can clearly be seen in the trajectories of Twizy 2 for both controllers. However, for both controllers Twizy 2 starts turning to the right, while Twizy 1 is driving straight. For the extended look-ahead controller from [1] it is observed that Twizy 2 tracks Twizy 1 well between $x = 35$ m and $x = 50$ m, but then Twizy 2 corners too late and subsequently it corners too early. For the developed controller it can be seen that Twizy 2 does not track Twizy 1 well initially. The vehicle is cornering while Twizy 1 is driving straight and after that Twizy 2 corners too late. From $x = 50$ m it can be seen that tracking of Twizy 2 improves. Overall it can be concluded that Twizy 2 is able to follow Twizy 1 for the slalom trajectory for both controllers.
In Figure 4.9 the tracking error can be seen for the slalom trajectory with both controllers and in Figure 4.10 the longitudinal and lateral errors can be seen for both controllers. For both controllers variations in the tracking error can be seen, the tracking error remains below 3.2 m initially but at the end a peak of 4.7 m is observed for the extended look-ahead controller from [1] and a peak of 4.3 m is observed for the developed controller. It can be seen that the longitudinal error oscillates around zero for both controllers. The RMS tracking error for the extended look-ahead controller from [1] is 1.94 m and the RMS tracking error of the developed controller is 1.76 m. The RMS tracking error of the developed controller is smaller than the RMS tracking of the extended look-ahead controller from [1], however both RMS tracking errors are significant.

4.3.3 Trajectory with a right-hand turn

In this scenario Twizy 1 starts from standstill and accelerates with 1 m/s^2 to 5 m/s. After 8 seconds Twizy 1 makes a right-hand turn and the vehicle is stopped when it reaches the end of the road. For this scenario a standstill distance r_i of 8 m and a time-gap h_i of 1 s are chosen. Again Twizy 2 is positioned without an initial spacing error behind Twizy 1.

In Figure 4.11 the trajectories of both vehicles can be seen for both controllers. From the figure it can be observed that with both controllers Twizy 2 turns left and right again, while Twizy 1 is driving straight. However, with both controller tracking improves at $x = 20$ m and from that moment the vehicle follows Twizy 1 well. It can be seen that with the extended look-ahead controller from [1] Twizy 2 stops next to the trajectory of Twizy 1, while Twizy 2 stops at the trajectory of Twizy 1 with the developed controller.
In Figure 4.12 the tracking error for controllers can be seen and in Figure 4.13 the longitudinal and lateral error for Twizy 2 can be seen. From the figures it can be seen that there is a peak in the tracking error at 6 seconds for both controllers, this peak is for both controllers mainly caused by the lateral error component. This lateral error can clearly be seen in Figure 4.11, since Twizy 2 steers to the right, while Twizy 1 is driving straight. At that moment the trajectory of Twizy 1 is on the left-side of Twizy 2, which results in a positive lateral error. After this peak the tracking error decreases for both controller and tracking improves. The RMS tracking errors are 1.40 m and 1.08 m for the extended look-ahead controller from [1] and the developed controller respectively. Again it can be observed that the RMS tracking error of the developed controller is smaller than the RMS tracking error of the extended look-ahead controller from [1].

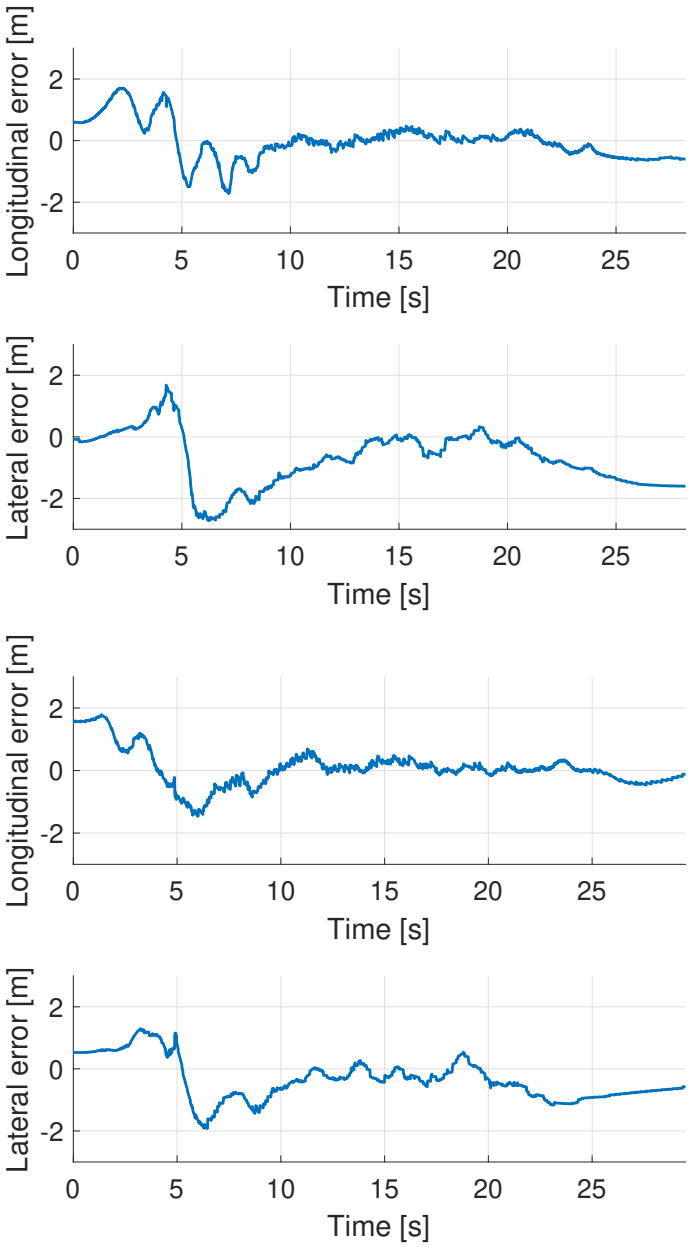

Figure 4.7: The longitudinal and lateral tracking error of Twizy 2: extended look-ahead controller from [1] (top) and the developed extended look-ahead controller (bottom).

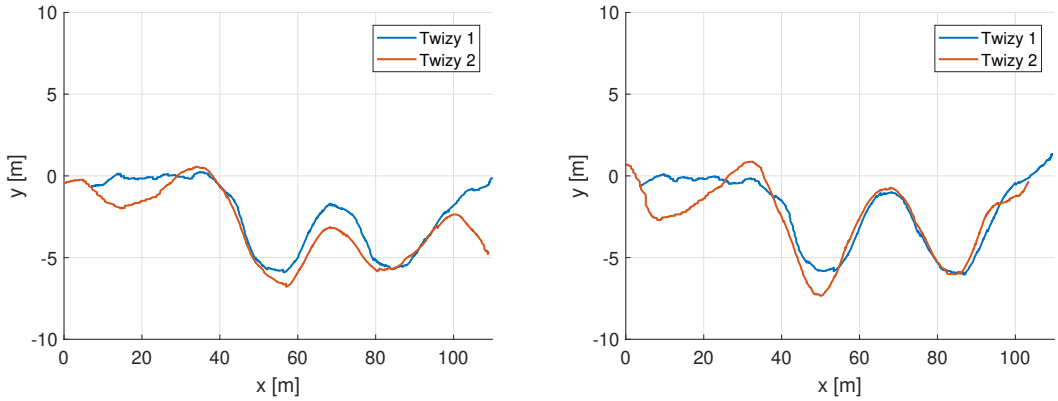

Figure 4.8: Trajectory of the Twizys: extended look-ahead controller from [1] (left) and the developed extended look-ahead controller (right).

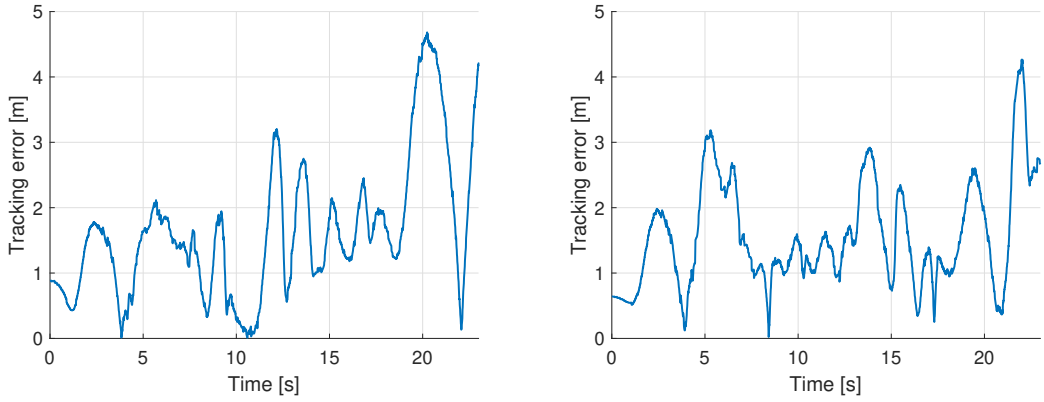

Figure 4.9: Tracking error of Twizy 2: extended look-ahead controller from [1] (left) and the developed extended look-ahead controller (right).

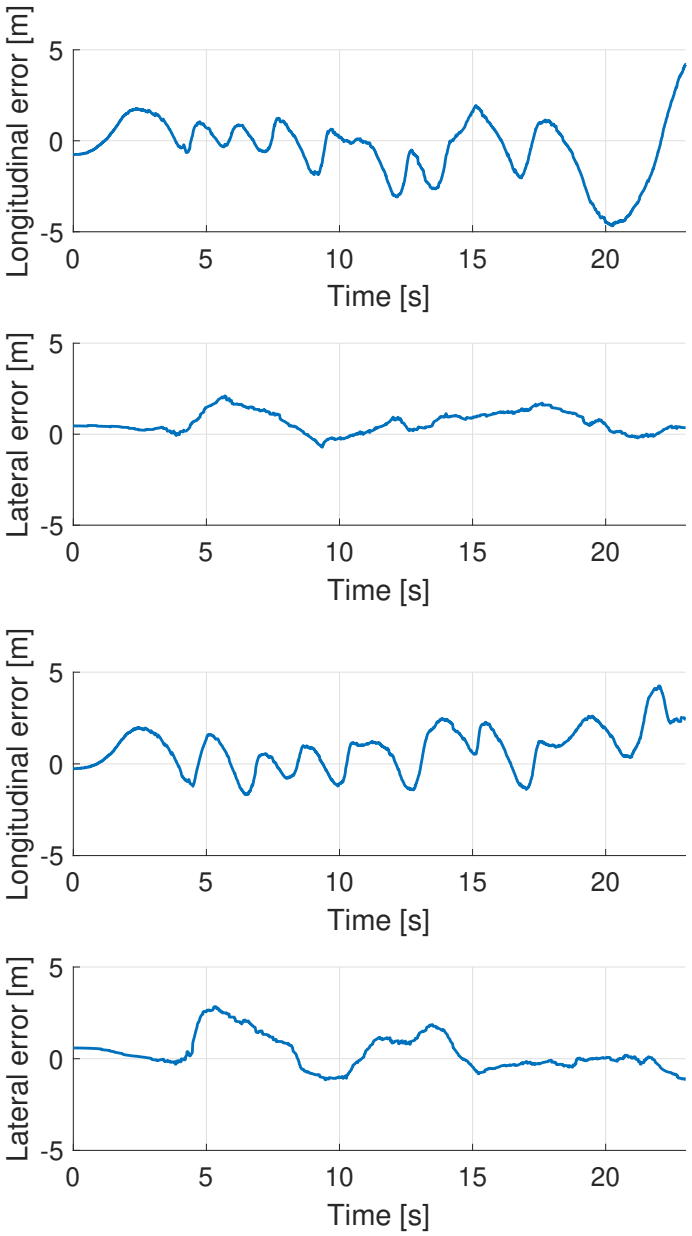

Figure 4.10: The longitudinal and lateral tracking error of Twizy 2: extended look-ahead controller from [1] (top) and the developed extended look-ahead controller (bottom).

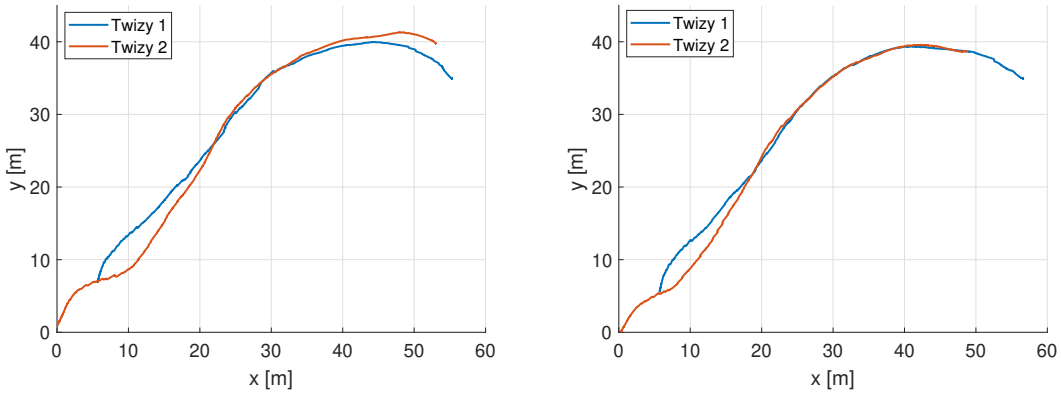

Figure 4.11: Trajectory of the Twizys: extended look-ahead controller from [1] (left) and the developed extended look-ahead controller (right).

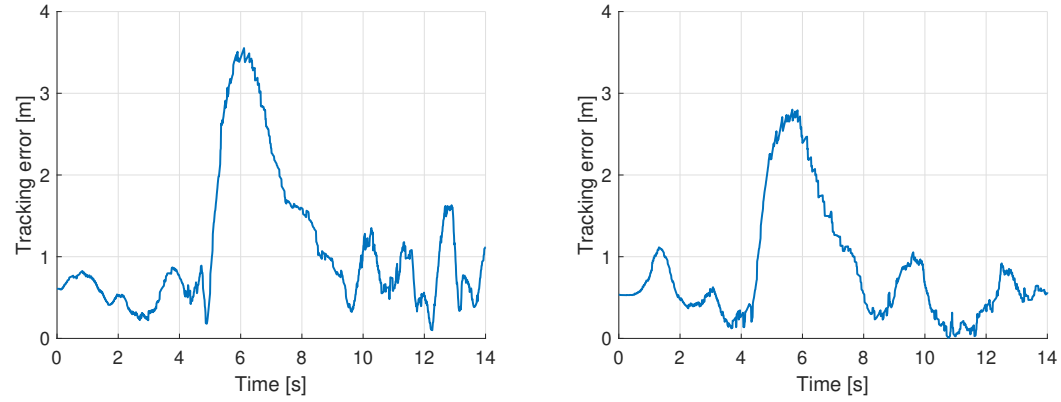

Figure 4.12: Tracking error of Twizy 2: extended look-ahead controller from [1] (left) and the developed extended look-ahead controller (right).

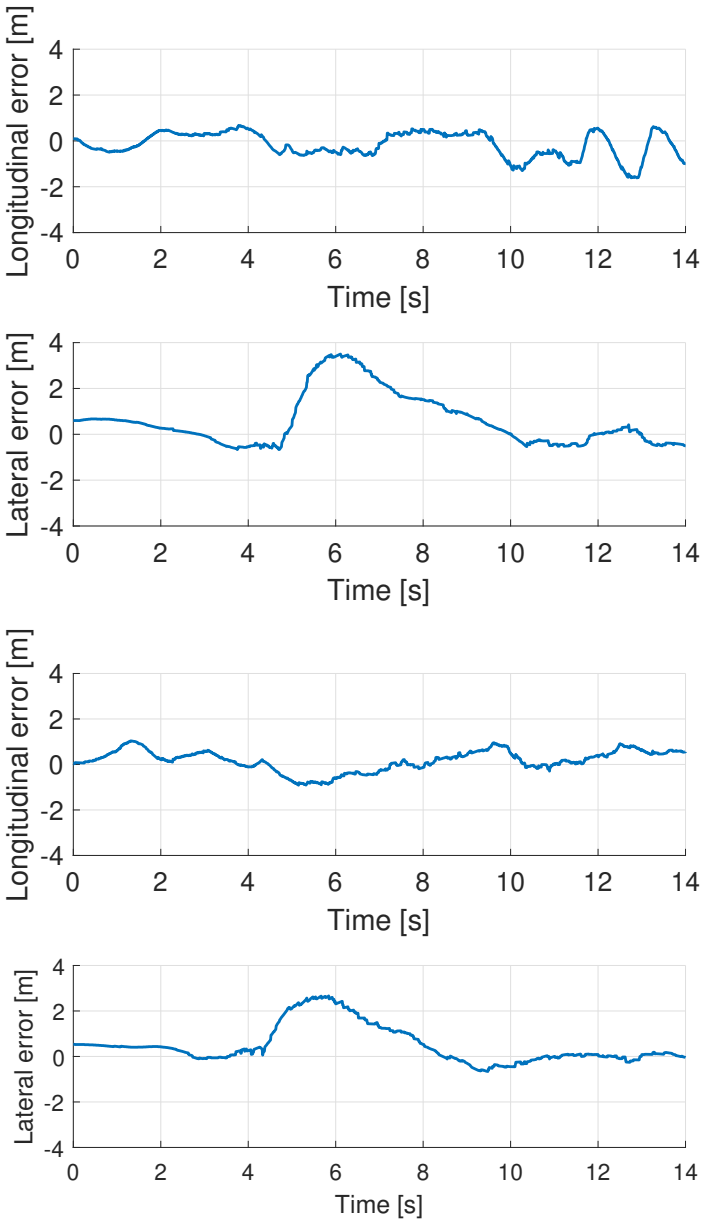

Figure 4.13: The longitudinal and lateral tracking error of Twizy 2: extended look-ahead controller from [1] (top) and the developed extended look-ahead controller (bottom).

4.4 Discussion

In the previous section the results from the experiments with the Renault Twizys are discussed. Results show that both controllers do actually work in the Renault Twizy and with these controllers it is possible to follow the preceding vehicle by only using the on-board sensors and vehicle-to-vehicle communication. Three different trajectories are tested and results show that the RMS tracking error does not exceed 1.94 m for the extended look-ahead controller from [1] and 1.76 m for the developed controller. The goal of the experiments is to test the controllers and to point out the differences and similarities between the simulations and the experiments. However, no clear conclusions can be drawn from the experimental results and we cannot state that the developed controller maintains the effective inter-vehicle distance nor that one of the controllers successfully compensate for corner-cutting behaviour. But what stands out is that Twizy 2 is able to follow Twizy 1 for all tested trajectories and that the tracking error remains bounded for both controllers, so we can conclude that both controllers do actually work in the Renault Twizys.

The main cause of the tracking error are the on-board sensors. Both controllers are developed in a global coordinate system, this means that both controllers heavily depend on accurate global position and heading measurements of the vehicles. However, the accuracy of a commercial GPS is about 5-15 meters [1]. The low accuracy of the GPS affects the behaviour of the controller, since the position errors are calculated by using the global positions provided by the GPS. These position errors are an input for the controller. An example can be seen in Figure 4.4, where the vehicles are driving a straight trajectory. Twizy 1 is driven manually, so small deviations from driving a straight line can be expected. However, from the GPS data it seems like Twizy 1 is cornering, this is caused by the poor accuracy of the GPS.

Furthermore, the state-estimator from [33] is used, but the state-estimator needs time to initialize while driving. Unfortunately, it is not possible to switch between manually driving and driving autonomously while driving. This means that during the first seconds of each measurement the state-estimator is still initializing, which affects the data that is used as an input for the controller. Another problem is that the heading of the vehicles drifts when the vehicles are standing still, this can clearly be seen in Figure 4.14. In the figure the vehicles are driving the straight trajectory and Twizy 1 did not corner. However, during the first 5 seconds a steep increase in the heading can be seen for both vehicles and after 5 seconds the heading stabilizes around -130 degrees. So, it can be concluded that the state-estimator requires time to initialize. This means that during the first seconds the data is not accurate yet and this affects the performance as can be seen in the experimental results. In all three scenarios Twizy 1 starts driving a straight line, however in each measurement it can be seen that Twizy 2 immediately starts cornering. In addition, the results presented in [33] are results in steady-state. During the experiment the vehicles are driving steady-state for only a short period of time.

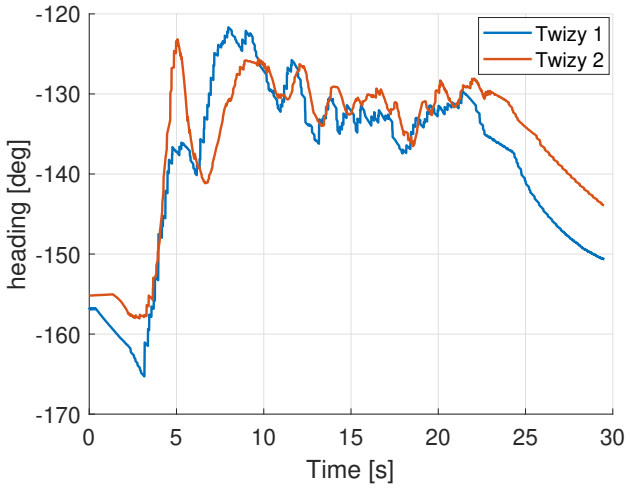

Figure 4.14: The heading of both vehicles for the straight trajectory.

4.5 Conclusions

In this section the practical set-up is discussed. The implementation of the extended look-ahead controller from [1] and the developed controller is described. Vehicle-to-vehicle wireless communication is implemented to communicate the relevant vehicle states and kinematic steering is used to convert the yaw-rate controller output into a steering angle. A control panel is designed to be able to make real-time changes in the control parameters. Experiments with two Renault Twizys are performed, where three different trajectories are tested: a straight trajectory, a slalom trajectory and a trajectory with a turn to the right. Twizy 1 is driven manually and the extended look-ahead controller from [1] and the developed controller are applied on Twizy 2. Results show that it is possible to follow Twizy 1 with both controllers and that the tracking error remains bounded. However, from the results it cannot be concluded that the developed controller maintains the effective inter-vehicle distance during cornering or that the extended look-ahead controller from [1] decreases the inter-vehicle distance during cornering. From the results it also cannot be seen that one of the controllers successfully compensate for corner-cutting behaviour.

Chapter 5

Conclusions and recommendations

The conclusions of this research are given in this final chapter as well as recommendations for future research. The objective for this thesis is to design a controller for longitudinal and lateral vehicle tracking, which improves tracking performance.

5.1 Conclusions

For combined longitudinal and lateral vehicle automation two approaches are considered: the path following method and the direct vehicle following method. The purpose of vehicle platooning is to increase the capacity of the roads and this is achieved by adopting a small inter-vehicle distance. However, the camera-based vision system that is often used in the path following method is not able to detect the lane markings when the vehicle is driving close to its preceding vehicle and sometimes lane markings are not even available. Alternative approaches that are often used in the path following method require costly modifications to vehicles and infrastructure, for example embedding roads with magnetic markers or equip vehicles with an RTK-GPS. An alternative is the direct vehicle method, this method does not require path information or lane markings. The direct vehicle method utilizes the already available information from CACC and is therefore considered as a cost-friendly approach. The direct vehicle method is used to design the controller in this research.

In the direct vehicle method the vehicle does not receive any path information and the challenge is to directly follow the preceding vehicle by using information from on-board sensors and vehicle-to-vehicle communication. However, corner-cutting behaviour is observed for controllers based on the look-ahead approach. In the case of corner-cutting the follower vehicle drives in a smaller radius than the preceding vehicle. An extended look-ahead point can be used to compensate for this corner-cutting behaviour. During cornering maneuvers a virtual vehicle extends from the base of the preceding vehicle and acts as tracking objective for the follower vehicle. The magnitude of this extension vector needs to be carefully chosen in order to prevent corner-cutting behaviour. However, with the extended look-ahead controller variations in inter-vehicle distance are observed during cornering maneuvers, which lead to undesired accelerations in longitudinal direction.

It is demonstrated that the effective inter-vehicle distance decreases during corner maneuvers with the extended look-ahead controller and this problem worsens for a decreasing turning radius and an increasing time-gap between the vehicles. Therefore, an extended look-ahead controller is designed that compensates for corner-cutting behaviour, while maintaining the effective inter-vehicle distance. For the controller the vehicles are modelled as unicycles in a global coordinate system. Modifications are made to the distance along the path between the vehicles and the projection of the extended look-ahead point to overcome the mentioned problems. This results in a controller that requires the following signals: the global positions of both vehicles, the velocity of both vehicles, the yaw-rate of the preceding vehicle and the heading of both vehicles. The states of

the preceding vehicle are obtained via vehicle-to-vehicle communication. Stability of the overall system is established for the case where the platoon is driving on a straight trajectory and for the case where the platoon is driving on a circular trajectory with a constant curvature and a constant velocity.

Simulations are performed to analyse the performance of the controller. To analyse the behaviour of the controller a measure for tracking performance is defined. A moving frame is attached to the follower vehicle, which ensures that the local x-axis corresponds to the longitudinal direction of the follower vehicle and the local y-axis corresponds to the lateral direction of the follower vehicle. Subsequently, the position of the preceding vehicle is backtransformed with a distance of $r_i + h_i v_i$ and the obtained position is compared with the actual position of the follower vehicle. This results in an accurate and measurable tracking performance measure. Simulations are performed for the case where the platoon is driving on a straight trajectory, here the developed controller behaves the same as the already existing extended look-ahead controller, which is as expected. For the scenario where the platoon enters a double lane roundabout it is observed that the developed controller successfully compensates for corner-cutting and that the effective-inter vehicle distance is maintained. While the already existing extended look-ahead controller only compensates for corner-cutting.

The already existing extended look-ahead controller and the developed controller are implemented in modified Renault Twizys for experiments. The leader vehicle is driven manually, while the controllers are applied on the follower vehicle. Three trajectories are defined: a straight trajectory, a slalom trajectory and a trajectory with a right-hand turn. Results show that the controllers are successfully implemented in the Renault Twizys, the follower vehicle is able to actually follow the leader vehicle. The tracking error remains bounded, but from the results it cannot be stated the effective inter-vehicle distance is maintained nor that corner-cutting behaviour is compensated.

To conclude, a control approach is developed that compensates for corner-cutting behaviour and that maintains the effective inter-vehicle distance during cornering maneuvers. A measurable tracking performance measure that analyses how well the follower vehicle tracks the leader vehicle is defined and the designed controller is successfully implemented in the Renault Twizys. As a result, an extended look-ahead controller for longitudinal and lateral vehicle tracking is designed, which improves tracking performance during cornering maneuvers. However, several areas of this research could serve improvements, which are explained in the following recommendation section.

5.2 Recommendations

Based on the results and the obtained insights the following recommendations are given:

The designed controller is developed in a global coordinate system. Simulations show promising results and in simulations this controller performs well on both straight trajectories and trajectories which have corners. However, the developed controller heavily depends on accurate global position measurements and measurements of the heading of the vehicles. Commercial vehicles are not equipped with an RTK-GPS and a commercial GPS has a poor accuracy. During the experiments it is observed that vehicle tracking is possible with the developed controller, but improvements are possible. The simplest solution is to equip every vehicle with an RTK-GPS, however this solution is very costly. A more sustainable solution is to adapt the developed controller in a local coordinate system. When the controller is developed in a local coordinate system the controller needs the relative position of the vehicles instead of using the global positions of the vehicles. The relative position can be measured with a camera or lidar and the relevant vehicle states can be communicated via vehicle-to-vehicle communication. Lidar or camera vision systems are already available in commercial vehicles, therefore this is considered as a cost-effective solution.

In simulations it is seen that the follower vehicle steers slightly away from the preceding vehicle before it enters the actual corner. This is caused by the definition of the extended look-ahead point. When the leader vehicle is driving on a straight trajectory along the positive x-axis and starts cornering to the left, the look-ahead point is extended, but when the leader vehicle did not made significant lateral movement this extended look-ahead point is positioned below the positive global x-axis. This causes the follower vehicle to steer in the opposite direction of the corner, since this extended look-ahead point acts as the new tracking objective for the follower vehicle. An adaptation in the definition of the extended look-ahead point which solves this problem needs to be developed. This would significantly improve tracking performance of the controller, since the tracking error of the developed controller is mainly caused by the described lateral error.

In this research the focus is on designing a controller that improves tracking performance of a vehicle platoon during cornering maneuvers. By using the proposed tracking performance measure it is demonstrated that the developed controller maintains the effective inter-vehicle distance and that it compensates for corner-cutting behaviour. However, string stability of the platoon is not analysed in this research. While string stability is an important criterion in vehicle platooning, string stability can be used to analyse if disturbances are amplified when propagating downstream along the vehicle string. Longitudinal and lateral string stability can be analysed separately, however a controller for both longitudinal and lateral vehicle tracking is developed. Therefore, it makes sense to analyse longitudinal and lateral string stability simultaneously. In [35] longitudinal and lateral string stability is analysed simultaneously by using mesh stability. Mesh stability is an extension of string stability, where stability is analysed in only one direction. In this method a mesh of vehicles is considered, where the desired positions of the vehicles in the mesh are known. The spacing error of the vehicles with respect to desired positions are determined and an error propagation relation is derived. This method can be used in vehicle platooning, however the mesh spacing errors need to be redefined, since the platoon does not drive in a mesh formation.

During the experiments we had practical problems with the Renault Twizys. The system often has a CPU overload, which results in lost experimental data and as a consequence the model has to be built again. Building the model takes a lot of time and the test track was available for a limited amount of time. Furthermore, there are problems with connecting the Simulink model with the Renault Twizys. A solution for the listed problems needs to be found in order to smoothly perform the experiments

Bibliography

[1] A. Bayuwindra. *Look-ahead tracking controllers for integrated longitudinal and lateral control of vehicle platoons*. PhD thesis, Department of Mechanical Engineering, Oct. 2019.

[2] Unfallentwicklung auf deutschen strassen 2017. https://www.destatis.de/DE/Presse/Pressekonferenzen/2018/Verkehrsunfaelle-2017/pressebroschuere-unfallentwicklung.pdf?__blob=publicationFile. (Accessed: 22-05-2021).

[3] ERSO. Advanced driver assistance systems. 2016.

[4] F. Browand, J. Mcarthur, and C. Radovich. Fuel saving achieved in the field test of two tandem trucks. *Institute of Transportation Studies, UC Berkeley, Institute of Transportation Studies*, Jan. 2004.

[5] R. Rajamani, H. Tan, B. Law, and W. Zhang. Demonstration of integrated longitudinal and lateral control for the operation of automated vehicles in platoons. *IEEE Transactions on Control Systems Technology*, 8(4):695–708, 2000.

[6] J. Bom, B. Thuilot, F. Marmoiton, and P. Martinet. A global control strategy for urban vehicles platooning relying on nonlinear decoupling laws. Sept. 2005.

[7] Ö. Tunçer, L. Güvenç, F. Coşkun, and E. Karslıgil. Vision based lane keeping assistance control triggered by a driver inattention monitor. In *2010 IEEE International Conference on Systems, Man and Cybernetics*, pages 289–297, 2010.

[8] P. Petrov. A mathematical model for control of an autonomous vehicle convoy. Jan. 2008.

[9] i-cave. https://i-cave.nl/. (Accessed: 06-01-2022).

[10] H. Nijmeijer, T. van der Sande, E. Klerks, G. Notten, and J. van der Sar. The future of moving forward. 2021.

[11] Oica 2019 production statistics. http://www.oica.net/category/production-statistics/2019-statistics/. (Accessed: 26-03-2021).

[12] P. Tientrakool, Y. Ho, and N. Maxemchuk. Highway capacity benefits from using vehicle-to-vehicle communication and sensors for collision avoidance. In *2011 IEEE Vehicular Technology Conference (VTC Fall)*, 2011.

[13] Commission of the European communities. The intelligent car initiative : Raising awareness of ict for smarter, safer and cleaner vehicles. Technical report, Brussels, 2006.

[14] J. Ploeg, N. Wouw, and H. Nijmeijer. Lp string stability of cascaded systems: Application to vehicle platooning. *IEEE Transactions on Control Systems Technology*, 22:786–793, Mar. 2014.

[15] D. Ren, J. Zhang, and C. Du. Variable structure adaptive control for vehicle longitudinal following in a platoon. In *2007 IEEE International Conference on Robotics and Biomimetics (ROBIO)*, pages 1906–1910, 2007.

[16] S. Sheikholeslam and C. Desoer. Longitudinal control of a platoon of vehicles. In *1990 American Control Conference*, pages 291–296, 1990.

[17] D. Swaroop and J. Hedrick. Constant Spacing Strategies for Platooning in Automated Highway Systems. *Journal of Dynamic Systems, Measurement, and Control*, 121(3):462–470, Sept. 1999.

[18] O. Gehring and H. Fritz. Practical results of a longitudinal control concept for truck platooning with vehicle to vehicle communication. In *Proceedings of Conference on Intelligent Transportation Systems*, pages 117–122, 1997.

[19] J. Zhao, M. Oya, and A. El Kamel. A safety spacing policy and its impact on highway traffic flow. In *2009 IEEE Intelligent Vehicles Symposium*, pages 960–965, 2009.

[20] J. Eyre, D. Yanakiev, and I. Kanellakopoulos. A simplified framework for string stability analysis of automated vehicles. *Vehicle System Dynamics*, 30(5):375–405, 1998.

[21] S. Feng, Y. Zhang, S. Li, Z. Cao, H. Liu, and L. Li. String stability for vehicular platoon control: Definitions and analysis methods. *Annual Reviews in Control*, 47:81–97, 2019.

[22] T. van der Sande and J. Ploeg. Lecture slides in vehicle dynamics, May. 2019.

[23] S. Shladover, C. Desoer, J. Hedrick, M. Tomizuka, J. Walrand, W. Zhang, D. Mcmahon, P. Huei, S. Sheikholeslam, and N. Mckeown. Automatic Vehicle Control Developments in the Path Program. *IEEE Transactions on Vehicular Technology*, 40(1, 1):114–130, Feb. 1991.

[24] H. Peng and M. Tomizuka. Vehicle lateral control for highway automation. In *1990 American Control Conference*, pages 788–794, 1990.

[25] T. Hessburg and M. Tomizuka. Fuzzy logic control for lateral vehicle guidance. *IEEE Control Systems Magazine*, 14(4):55–63, 1994.

[26] J. Hedrick, M. Tomizuka, and P. Varaiya. Control issues in automated highway systems. *IEEE Control Systems Magazine*, 14(6):21–32, 1994.

[27] V. Cerone, A. Chinu, and D. Regruto. Experimental results in vision-based lane keeping for highway vehicles. In *Proceedings of the 2002 American Control Conference*, volume 1-6 of *Proceedings of the American Control Conference*, pages 869–874, 2002.

[28] V. Cerone, M. Milanese, and D. Regruto. Combined automatic lane-keeping and driver's steering through a 2-dof control strategy. *IEEE Transactions on Control Systems Technology*, 17(1):135–142, 2009.

[29] Y. Son, W. Kim, S. Lee, and C. Chung. Robust Multirate Control Scheme With Predictive Virtual Lanes for Lane-Keeping System of Autonomous Highway Driving. *IEEE Transactions on Vehicular Technology*, 64(8):3378–3391, Aug 2015.

[30] S. Solyom, A. Idelchi, and B. Salamah. Lateral control of vehicle platoons. Oct. 2013.

[31] Royal Haskoning. Roundabouts - application and design. Jun. 2009.

[32] F. Hoogeboom. *Safety of automated vehicles: design, implementation, and analysis.* PhD thesis, Mechanical Engineering, Oct 2020.

[33] W. Schinkel, T. van der Sande, and H. Nijmeijer. State estimation for cooperative lateral vehicle following using vehicle-to-vehicle communication. *Electronics*, 10(6), Mar. 2021.

[34] D. Schramm, M. Hiller, and R. Bardini. *Single Track Models*, pages 223–253. Springer Berlin Heidelberg, Berlin, Heidelberg, 2014.

[35] A. Pant, P. Seiler, T. J. Koo, and K. Hedrick. Mesh stability of unmanned aerial vehicle clusters. In *Proceedings of the 2001 American Control Conference*, volume 1, pages 62–68, 2001.

Appendix A

Appendix chapter 3

A.1 Stability analysis of the developed extended look-ahead controller

In this section the stability of the internal dynamics is analysed. Here two cases are considered, the first case is when the platoon maneuvers on a straight trajectory and the second case is where the platoon maneuvers on a circular trajectory with a constant curvature and a constant velocity.

A.1.1 Case 1: straight line

In this section the case where the platoon maneuvers on a straight line is analysed. This means that $\omega_{i-1} = 0$, $\kappa_{i-1} = 0$, $\dot{\kappa}_{i-1} = 0$ and $\alpha_i = 0$. Let $z_{34,i} = [z_{3,i}, z_{4,i}]^T$. For this case the dynamics from (3.50) can be rewritten as:

$$\begin{bmatrix} \dot{z}_{3,i} \\ \dot{z}_{4,i} \end{bmatrix} = -\begin{bmatrix} \frac{h_i v_i + r_i \cos^2\theta_i}{h_i(r_i+h_i v_i)} & \frac{r_i \sin\theta_i \cos\theta_i}{h_i(r_i+h_i v_i)} \\ \frac{r_i \sin\theta_i \cos\theta_i}{h_i(r_i+h_i v_i)} & \frac{h_i v_i + r_i \sin^2\theta_i}{h_i(r_i+h_i v_i)} \end{bmatrix} \begin{bmatrix} z_{3,i} \\ z_{4,i} \end{bmatrix} + \xi_i \tag{A.1}$$

Where

$$\begin{aligned} \begin{bmatrix} \xi_{1,i} \\ \xi_{2,i} \end{bmatrix} := & \begin{bmatrix} \cos\theta_{i-1} & -v_{i-1}\sin\theta_{i-1} \\ \sin\theta_{i-1} & v_{i-1}\cos\theta_{i-1} \end{bmatrix} \begin{bmatrix} a_{i-1} \\ \omega_{i-1} \end{bmatrix} \\ & - \begin{bmatrix} \frac{h_i v_i + r_i \cos^2\theta_i}{h_i(r_i+h_i v_i)} & \frac{r_i \sin\theta_i \cos\theta_i}{h_i(r_i+h_i v_i)} \\ \frac{r_i \sin\theta_i \cos\theta_i}{h_i(r_i+h_i v_i)} & \frac{h_i v_i + r_i \sin^2\theta_i}{h_i(r_i+h_i v_i)} \end{bmatrix} \begin{bmatrix} k_1 z_{1,i} \\ k_2 z_{2,i} \end{bmatrix} \end{aligned} \tag{A.2}$$

This subsystem is exactly the same as in [1], which is as expected. When the platoon is driving on a straight line the behaviour of the developed extended look-ahead controller is exactly the same as the extended look-ahead controller from [1]. Therefore, it can be concluded from [1] that $\lim_{t\to\infty} ||z_{34,i}(t)|| = 0$ and thus the straight line case is stable.

A.1.2 Case 2: circular trajectory with a constant curvature and a constant velocity

In this subsection the case where the platoon maneuvers on a circular trajectory with a constant curvature and a constant velocity is considered. for $\kappa_{i-1} \neq 0$ the dynamics from (3.50) can be rewritten as:

$$\begin{bmatrix} \dot{z}_{3,i} \\ \dot{z}_{4,i} \end{bmatrix} = -\frac{1}{\lambda_i h_i} \begin{bmatrix} p_{11} & p_{12} \\ p_{21} & p_{22} \end{bmatrix} \begin{bmatrix} z_{3,i} \\ z_{4,i} \end{bmatrix} - \kappa_{i-1} \left(Q_i \begin{bmatrix} z_{3,i} \\ z_{4,i} \end{bmatrix} - f_{v,i} \right) + \zeta_i \tag{A.3}$$

Where

$$f_{v,i} = \begin{bmatrix} -v_{i-1}\sin\theta_{i-1} \\ v_{i-1}\cos\theta_{i-1} \end{bmatrix} v_{i-1} - \begin{bmatrix} -v_i\sin(\theta_i+\alpha_i) \\ v_i\cos(\theta_i+\alpha_i) \end{bmatrix} v_i \tag{A.4}$$

$$\zeta_i = h_{\kappa,i}\dot{\kappa}_{i-1} + \begin{bmatrix} \cos\theta_{i-1} \\ \sin\theta_{i-1} \end{bmatrix} a_{i-1} - \Gamma_{34,i}\Gamma_{12,i}^{-1}\begin{bmatrix} k_1 z_{1,i} \\ k_2 z_{2,i} \end{bmatrix} \tag{A.5}$$

$$\begin{aligned} h_{\kappa,i} =& v_i\left(r_i + h_i v_i\right)\begin{bmatrix} \sin(\theta_i+\alpha_i) \\ -\cos(\theta_i+\alpha_i) \end{bmatrix} + \Gamma_{34}\Gamma_{12}^{-1}\left(\frac{-\tan\alpha_i}{\kappa_{i-1}^2} + \frac{r_i+h_i v_i}{\kappa_{i-1}\cos^2\alpha_i}\right)\begin{bmatrix} \cos\theta_i \\ \sin\theta_i \end{bmatrix} \\ &- \Gamma_{34}\Gamma_{12}^{-1}\left(\frac{1-\sec\alpha_i}{\kappa_{i-1}^2} + \frac{(r_i+h_i v_i)\tan\alpha_i}{\kappa_{i-1}\cos\alpha_i}\right)\begin{bmatrix} \sin\theta_{i-1} \\ -\cos\theta_{i-1} \end{bmatrix} \end{aligned} \tag{A.6}$$

$$\begin{aligned} p_{11} &= \cos^2\alpha_i\cos\theta_i\cos(\theta_i+\alpha_i) \\ p_{12} &= \cos^2\alpha_i\sin\theta_i\cos(\theta_i+\alpha_i) \\ p_{21} &= \cos^2\alpha_i\cos\theta_i\sin(\theta_i+\alpha_i) \\ p_{22} &= \cos^2\alpha_i\sin\theta_i\sin(\theta_i+\alpha_i) \end{aligned} \tag{A.7}$$

$$Q_i = \frac{v_i}{\lambda_i}\begin{bmatrix} q_{11} & q_{12} \\ q_{21} & q_{22} \end{bmatrix} \tag{A.8}$$

$$\lambda_i = 1 - \sin\alpha_i\sin(\theta_{i-1}-\theta_i) \tag{A.9}$$

$$\begin{aligned} q_{11} &= \sin(\theta_i+\alpha_i)(-\cos^3\alpha_i\cos\theta_i + \cos\theta_{i-1} + \frac{\sin\theta_i}{\sin\alpha_i}) \\ q_{12} &= \sin(\theta_i+\alpha_i)(-\cos^3\alpha_i\sin\theta_i + \sin\theta_{i-1} - \frac{\cos\theta_i}{\sin\alpha_i}) \\ q_{21} &= \cos(\theta_i+\alpha_i)(\cos^3\alpha_i\cos\theta_i - \cos\theta_{i-1} - \frac{\sin\theta_i}{\sin\alpha_i}) \\ q_{22} &= \cos(\theta_i+\alpha_i)(\cos^3\alpha_i\sin\theta_i - \sin\theta_{i-1} + \frac{\cos\theta_i}{\sin\alpha_i}) \end{aligned} \tag{A.10}$$

Now we assume that $0 < \varepsilon < v_{i-1}^{\min} \leq v_{i-1} \leq v_{i-1}^{\max}$ and we take the set $\Omega_c = \{||z_{34,i}|| \leq v_{i-1}^{\min} - \varepsilon\}$. Inside the set Ω_c we have that:

$$\begin{aligned} \varepsilon^2 &\leq (v_{i-1}^{\min} - ||z_{34,i}||)^2 \leq (v_{i-1} - ||z_{34,i}||)^2 \\ &= v_{i-1}^2 - 2v_{i-1}\sqrt{z_{3,i}^2 + z_{4,i}^2} + z_{3,i}^2 + z_{4,i}^2 \end{aligned} \tag{A.11}$$

Now we can use the Cauchy-Schwarz inequality, which is defined as:

$$\begin{aligned} ||x+y||^2 &\leq ||x||^2 + 2||x||\,||y|| + ||y||^2 \\ -2||x||\,||y|| &\leq -||x+y||^2 + ||x||^2 + ||y||^2 \\ 2||x||\,||y|| &\geq ||x+y||^2 - ||x||^2 - ||y||^2 \end{aligned} \tag{A.12}$$

Now take $c = [\cos\theta_{i-1},\ \sin\theta_{i-1}]^T$ and use this in the Cauchy-Schwarz inequality. This results in:

$$\begin{aligned} 2||z_{34,i}||\,||c|| &\geq ||z_{34,i}+c||^2 - ||z_{34,i}||^2 - ||c||^2 \\ 2\sqrt{z_{3,i}^2 + z_{4,i}^2} &\geq 2z_{3,i}\cos\theta_{i-1} + 2z_{4,i}\sin\theta_{i-1} \end{aligned} \tag{A.13}$$

Substituting this into (A.11) yields:

$$\begin{aligned}\varepsilon^2 &\leq v_{i-1}^2 - 2v_{i-1}z_{3,i}\cos\theta_{i-1} - 2v_{i-1}z_{4,i}\sin\theta_{i-1} + z_{3,i}^2 + z_{4,i}^2 \\ &\leq (v_{i-1}\cos\theta_{i-1} - z_{3,i})^2 + (v_{i-1}\sin\theta_{i-1} - z_{4,i})^2 \\ &\leq v_i^2\end{aligned} \tag{A.14}$$

So, we can conclude that inside Ω_c it holds that $v_i(t) \geq \varepsilon > 0$. So the goal is to prove that when $||z_{34,i}(0)|| \leq v_{i-1}^{\min} - \varepsilon$ it will stay within Ω_c for every $t > 0$.

In this case we have that $a_{i-1} = 0$, $\dot{\kappa}_{i-1} = 0$, $z_1 = 0$ and $z_2 = 0$, which means that the term ζ_i is equal to zero. Now we need to find the Lyapunov function for the dynamics of z_3 and z_4.
The Lyapunov function $V = z_{3,i}^2 + z_{4,i}^2$ is used, the derivative of V with respect to time is: $\dot{V} = 2z_3\dot{z_3} + 2z_4\dot{z_4}$. Thus the derivative of V along (A.3) with respect to time is given by:

$$\begin{aligned}\dot{V} = &-\frac{2\cos^2\alpha_i}{\lambda_i h_i}\left(z_{3,i}\cos\left(\theta_i+\alpha_i\right) + z_{4,i}\sin\left(\theta_i+\alpha_i\right)\right)\left(z_{3,i}\cos\theta_i + z_{4,i}\sin\theta_i\right) \\ &+ \frac{2\kappa_{i-1}v_i\cos^3\alpha_i}{\lambda_i}\left(z_{3,i}\sin\left(\theta_i+\alpha_i\right) - z_{4,i}\cos\left(\theta_i+\alpha_i\right)\right)\left(z_{3,i}\cos\theta_i + z_{4,i}\sin\theta_i\right) \\ &- \frac{2\kappa_{i-1}v_i}{\lambda_i}\left(z_{3,i}\sin\left(\theta_i+\alpha_i\right) - z_{4,i}\cos\left(\theta_i+\alpha_i\right)\right)\left(z_{3,i}\cos\theta_{i-1} + z_{4,i}\sin\theta_{i-1}\right) \\ &- \frac{2\kappa_{i-1}v_i}{\lambda_i\sin\alpha_i}\left(z_{3,i}\sin\left(\theta_i+\alpha_i\right) - z_{4,i}\cos\left(\theta_i+\alpha_i\right)\right)\left(z_{3,i}\sin\theta_i - z_{4,i}\cos\theta_i\right) \\ &+ 2\kappa_{i-1}v_{i-1}\left(v_{i-1}-v_i\right)\left(-z_{3,i}\sin\theta_{i-1} + z_{4,i}\cos\theta_{i-1}\right)\end{aligned} \tag{A.15}$$

We can apply the Cauchy-Schwarz inequality to the terms in (A.15) that are dependent on $z_{3,i}$ and $z_{4,i}$. This results in that those terms are always less or equal to $||z_{34,i}||$. From (A.9) it follows that $\lambda_i \leq 2$ and applying the Cauchy-Schwarz inequality to (3.30) and (3.31) we find that $v_{i-1} - v_i \leq ||z_{34,i}||$. Applying this to (A.15) we find:

$$\begin{aligned}\dot{V} \leq &-\frac{\cos^2\alpha_i}{h_i}||z_{34,i}||^2 + \kappa_{i-1}v_i\cos^3\alpha_i||z_{34,i}||^2 - \kappa_{i-1}v_i||z_{34,i}||^2 \\ &- \frac{\kappa_{i-1}v_i}{\sin\alpha_i}||z_{34,i}||^2 + 2\kappa_{i-1}v_{i-1}||z_{34,i}||^2\end{aligned} \tag{A.16}$$

This equation can be rewritten as:

$$\dot{V} \leq -\left(\frac{\cos^2\alpha_i}{h_i} + \kappa_{i-1}(v_i(1+\frac{1}{\sin\alpha_i} - \cos^3\alpha_i) - 2v_{i-1})\right)||z_{34,i}||^2 \tag{A.17}$$

Which is negative for

$$\frac{\cos^2\alpha_i}{h_i} + \kappa_{i-1}(v_i(1+\frac{1}{\sin\alpha_i} - \cos^3\alpha_i) - 2v_{i-1}) > 0 \tag{A.18}$$

Thus

$$\frac{\cos^2\alpha_i}{h_i} - |\kappa_{i-1}|\,|(v_i(1+\frac{1}{\sin\alpha_i} - \cos^3\alpha_i) - 2v_{i-1})| > 0 \tag{A.19}$$

And it is sufficient to have:

$$\frac{\cos^2\alpha_i}{h_i} - |\kappa_{i-1}|\,|(v_i(1+\frac{1}{\sin\alpha_i} - \cos^3\alpha_i) - 2v_{i-1}^{\min})| > 0 \tag{A.20}$$

Which results in:

$$|\kappa_{i-1}| < \frac{\cos^2 \alpha_i}{h_i |v_i (1 + \frac{1}{\sin \alpha_i} - \cos^3 \alpha_i) - 2v_{i-1}^{\min}|} \tag{A.21}$$

From (3.30) and (3.31) it follows that:

$$\begin{aligned} v_i^2 &= (v_{i-1} \cos \theta_{i-1} - z_{3,i})^2 + (v_{i-1} \sin \theta_{i-1} - z_{4,i})^2 \\ &= v_{i-1}^2 + \|z_{34,i}\|^2 - 2v_{i-1} z_{3,i} \cos \theta_{i-1} - 2v_{i-1} z_{4,i} \sin \theta_{i-1} \\ &\leq v_{i-1}^2 + \|z_{34,i}\|^2 + z_{3,i}^2 + z_{4,i}^2 + v_{i-1}^2 \cos^2 \theta_{i-1} + v_{i-1}^2 \sin^2 \theta_{i-1} \\ &= 2v_{i-1}^2 + 2 \|z_{34,i}\|^2 \leq 2 \left(v_{i-1} + \|z_{34,i}\|\right)^2 . \end{aligned} \tag{A.22}$$

Which gives:

$$0 < \varepsilon \leq v_i \leq \sqrt{2} \left(v_{i-1}^{\max} + v_{i-1}^{\min} - \varepsilon\right) \tag{A.23}$$

By combining (A.21) and (A.23) we obtain:

$$\begin{aligned} |\kappa_{i-1}| &< \frac{\cos^2 \alpha_i}{h_i |\sqrt{2} \left(v_{i-1}^{\max} + v_{i-1}^{\min} - \varepsilon\right) (1 + \frac{1}{\sin \alpha_i} - \cos^3 \alpha_i) - 2v_{i-1}^{\min}|} \\ &\leq \frac{\cos^2 \alpha_i}{h_i |v_i (1 + \frac{1}{\sin \alpha_i} - \cos^3 \alpha_i) - 2v_{i-1}^{\min}|} \end{aligned} \tag{A.24}$$

Therefore, it can be concluded that if $||z_{34,i}(0)|| \leq v_{i-1}^{\min} - \varepsilon$, then it holds that $v_i(t) > 0$. Furthermore, for κ_{i-1} bounded within (A.24) we have that $\lim_{t \to \infty} ||z_{34,i}(t)|| = 0$ for the case where the platoon is driving on a trajectory with a constant curvature and a constant velocity.